



# 1 A comprehensive biogeochemical record and annual flux estimates 2 for the Sabaki River (Kenya)

3 Trent R. Marwick<sup>1</sup>, Fredrick Tamooh<sup>2</sup>, Bernard Ogwoka<sup>3</sup>, Alberto V. Borges<sup>4</sup>, François Darchambeau<sup>4</sup>,  
4 and Steven Bouillon<sup>1</sup>

5 <sup>1</sup> Department of Earth and Environmental Sciences, KU Leuven, Leuven, 3001, Belgium

6 <sup>2</sup> Kenyatta University, Department of Zoological Sciences, Mombasa, Kenya.

7 <sup>3</sup> Kenya Wildlife Service, Mombasa, Kenya

8 <sup>4</sup> Unité d'Océanographie Chimique, Université de Liège, Liège, 4000, Belgium

9 *Correspondence to:* Trent R. Marwick (trent.marwick@gmail.com)



1 **Abstract.** Inland waters impart considerable influence on nutrient cycling and budget estimates across local, regional and  
2 global scales, whilst anthropogenic pressures, such as rising populations and the appropriation of land and water resources,  
3 are undoubtedly modulating the flux of carbon (C), nitrogen (N), and phosphorus (P) between terrestrial biomes to inland  
4 waters, and the subsequent flux of these nutrients to the marine and atmospheric domains. Here, we present a two year  
5 biogeochemical record (Oct. 2011 – Dec. 2013) at bi-weekly sampling resolution for the lower Sabaki River, Kenya, and  
6 provide estimates for suspended sediment and nutrient export fluxes from the Athi-Galana-Sabaki (A-G-S) river basin under  
7 pre-dam conditions, and in light of the approved construction of the Thwake Multi-purpose Dam on the Athi River. Erratic  
8 seasonal variation was typical for most parameters, with generally poor correlation between discharge and material  
9 concentrations and stable isotopic signatures of C ( $\delta^{13}\text{C}$ ) and N ( $\delta^{15}\text{N}$ ). Although high total suspended matter (TSM)  
10 concentrations are reported here (up to  $\sim 3.8 \text{ g L}^{-1}$ ), peak concentrations of TSM rarely coincided with peak discharge. The  
11 contribution of particulate organic C (POC) to the TSM pool indicates a wide bi-annual variation in suspended sediment load  
12 from OC-poor (0.3%) to OC-rich (14.9%), with the highest %POC occurring when discharge is  $< 100 \text{ m}^3 \text{ s}^{-1}$  and at lower  
13 TSM concentrations. The consistent  $^{15}\text{N}$  enrichment of the PN pool compared to other river systems indicates anthropogenic  
14 N-loading is a year-round driver of N export from the A-G-S basin. The Sabaki River was consistently oversaturated in  
15 dissolved methane ( $\text{CH}_4$ ; from 499% to 135,111%) and nitrous oxide ( $\text{N}_2\text{O}$ ; 100% to 463%) relative to atmospheric  
16 concentrations. We estimate export fluxes to the coastal zone of  $4.0 \text{ Tg yr}^{-1}$ ,  $70.6 \text{ Gg C yr}^{-1}$ ,  $9.4 \text{ Gg N yr}^{-1}$ , and  $0.5 \text{ Gg P yr}^{-1}$  for TSM, POC, and particulate forms of N (PN) and total P (TPP), respectively, and fluxes of  $24.1 \text{ Gg C yr}^{-1}$ ,  $6.6 \text{ Gg N yr}^{-1}$ , and  $11.2 \text{ Gg P yr}^{-1}$  for dissolved forms of organic C (DOC), inorganic N (DIN), and phosphate ( $\text{PO}_4^{3-}$ ). Wet season  
17 flows (Oct. – Dec. and Mar. – May) carried  $> 80\%$  of the total load for TSM ( $\sim 86\%$ ), POC ( $\sim 89\%$ ), DOC ( $\sim 81\%$ ), PN  
18 ( $\sim 89\%$ ) and TPP ( $\sim 82\%$ ), with  $> 50\%$  of each fraction exported during the long wet season (Mar. – May). Our estimated  
19 sediment yield of  $85 \text{ Mg km}^{-2} \text{ yr}^{-1}$  is relatively low on the global scale and is considerably less than the recently reported  
20 average sediment yield of  $\sim 630 \text{ Mg km}^{-2} \text{ yr}^{-1}$  for African river basins. Regardless, sediment and OC yields were all at least  
21 equivalent or greater than reported yields for the neighbouring and flow-regulated Tana River. Rapid pulses of heavily  $^{13}\text{C}$ -  
22 enriched POC coincided with peak concentrations of PN, ammonium,  $\text{CH}_4$  and low dissolved oxygen saturation, lead to the  
23 suggestion that large mammalian herbivores (e.g. hippopotami) may mediate the delivery of  $\text{C}_4$  organic matter to the river  
24 during the dry season. Given recent projections for increasing dissolved nutrient export from African rivers, as well as  
25 planned flow regulation on the Athi River, these first estimates of material fluxes from the Sabaki River provide base-line  
26 data for future research initiatives assessing anthropogenic perturbation of the A-G-S river basin.

29 **Copyright statement**

30 The authors agree with the licence and copyright agreement.



## 1 1 Introduction

2 The acknowledgement of the vital role inland waters play in carbon (C) cycling and budget estimates at local, regional and  
3 global scales has progressed steadily over the past three decades (e.g. Likens et al., 1981; Meybeck, 1982; Hedges et al.,  
4 1986; Kling et al., 1991; Cole et al., 1994; Ludwig et al., 1996; Richey et al., 2002; Cole et al., 2007; Battin et al., 2008;  
5 Tranvik et al., 2009; Bastviken et al., 2011; Raymond et al., 2013; Borges et al. 2015a), advancing to the state where  
6 individual components of the C budget of inland waters are included and parameterised within the Intergovernmental Panel  
7 on Climate Change (IPCC) budgeting of the global C cycle (see IPCC, 2013; also Ciais et al., 2013). For example, inland  
8 waters not only act as a conduit for the delivery of significant quantities of terrestrial organic C to the coastal zone and open  
9 ocean, they are typically sources of greenhouse gases (GHG's, CO<sub>2</sub>, CH<sub>4</sub>, N<sub>2</sub>O) to the atmosphere, derived either from active  
10 heterotrophic metabolism remineralising a proportion of lateral inputs, through inputs from groundwaters and floodwaters  
11 which carry the products of mineralization in the terrestrial domain (Cole and Caraco, 2001a; Battin et al., 2009; Beaulieu et  
12 al., 2011; Raymond et al., 2013), or from wetlands (Abril et al. 2014; Borges et al. 2015a) with recent data compilations  
13 further elucidating the controls and drivers of GHG dynamics within the fluvial domain at regional and global scales (Borges  
14 et al., 2015a, Stanley et al., 2016, Marzadri et al., 2017). Additionally, a quantity of the lateral inputs may be buried within  
15 sedimentary deposits of reservoirs, lakes, floodplains and wetlands (Cole et al., 2007; Battin et al., 2008; Aufdenkampe et  
16 al., 2011). Anthropogenic pressures, such as land-use and land-use change, are undoubtedly modulating the quantities  
17 involved in each of these exchange fluxes (Regnier et al., 2013).

18 Given that recent reports assert a similar order of magnitude to the lateral C input to inland waters (~2.3 Pg C yr<sup>-1</sup>) as that for  
19 global net ecosystem production (~2 Pg C yr<sup>-1</sup>) (see Cole et al., 2007; Battin et al., 2009; Aufdenkampe et al., 2011; Ciais et  
20 al., 2013), the scarcity of the current empirical biogeochemical database for some regional inland waters is key to our  
21 inability to adequately resolve the role of this Earth System domain within broader regional and global C budgets (Raymond  
22 et al., 2013; Regnier et al., 2013). Although the spotlight has turned somewhat towards establishing a comprehensive  
23 reckoning of riverine C source variability and constraining C cycling within river basins, rather than solely quantifying the  
24 transport fluxes from inland waters to the coastal zone (Bouillon et al., 2012), there remain important inland water systems  
25 or regions lacking long-term, riverine biogeochemical datasets built upon high frequency sampling initiatives capable of  
26 providing reliable transport flux estimates. Tropical and sub-tropical Africa is one region where such datasets are scarce (e.g.  
27 Coynel et al., 2005; Borges et al. 2015a). On the global scale, the tropics and subtropics are considered of particular  
28 importance regarding the transport of sediments and C (Ludwig et al., 1996; Schlünz and Schneider, 2000; Moore et al.,  
29 2011), with a recent compilation of African sediment yield (hereafter, SY) data highlighting the paucity of observations  
30 relative to other continental regions (Vanmaercke et al., 2014). Also, the inland waters of the tropics and subtropics are  
31 suggested to have elevated evasion rates of CO<sub>2</sub> to the atmosphere in comparison to temperate and boreal inland waters  
32 (Aufdenkampe et al., 2011; Raymond et al., 2013; Borges et al. 2015a,b), and the same has been asserted for global CH<sub>4</sub> flux  
33 from tropical rivers and lakes (Bastviken et al., 2011; Borges et al. 2015a,b). Hence, given their reported significance as a



1 source of GHGs to the atmosphere, an increased focus on the inland water biogeochemistry of the tropics is merited (Regnier  
2 et al., 2013; Stanley et al., 2016), particularly for data-scarce river basins of Africa, given these regions contribute some of  
3 the largest uncertainty to global C budgets (Ciais et al., 2011).

4 Over the preceding decade, momentum has gathered towards a broader understanding of the nutrient cycling within sub-  
5 Saharan inland water ecosystems (e.g. Coynel et al., 2005; Brunet et al., 2009; Abrantes et al., 2013; Zurbrügg et al., 2013;  
6 Bouillon et al., 2014). Yet, Africa has experienced the highest annual population growth rate over the preceding 60 years  
7 (~2.51%, 1950 – 2013; see United Nations, 2013), a position it is expected to hold for the remainder of the 21<sup>st</sup> century  
8 (United Nations, 2013). Coupling the increasing population with forecasted climate change scenarios, land-use changes  
9 including deforestation and expanding agricultural practises, hydrological flow regulation through dam and reservoir  
10 construction and water abstraction, as well as increased exploitation of natural resources for food, fuel and wood products,  
11 will shift the dynamics of lateral nutrient inputs to inland waters of Africa, as well as the balance between transport and in-  
12 situ processing of these terrestrial subsidies, and consequently the regional C and nutrient balance of Africa (Hamilton, 2010;  
13 Yasin et al., 2010; Ciais et al., 2011; Valentini et al., 2014). Hence, continued effort in characterising the biogeochemistry of  
14 African inland waters is paramount for developing robust regional and global nutrient budgets, but also to provide a working  
15 baseline for assessing future climate and land-use impacts on the nutrient fluxes to and from inland waters of Africa.

16 The potential perturbation of the biogeochemistry of tropical inland waters by climate and land-use change (Hamilton,  
17 2010), and those of Africa specifically (Yasin et al., 2010), has received some attention. Given a projected warming of a ~2 –  
18 4.5 °C toward the end of the 21<sup>st</sup> century within the tropics (Meehl et al., 2007; Buontempo et al., 2015) and in East Africa  
19 specifically (Buontempo et al., 2015; Dosio and Panitz, 2016), important shifts are predicted involving: (i) aquatic thermal  
20 regime, influencing rates of in-situ microbe-mediated biogeochemical processes, (ii) hydrological regimes of discharge and  
21 floodplain inundation, and (iii) freshwater-saltwater gradients, altering biogeochemical processing as rivers approach the  
22 coastal zone. Additionally, Yasin et al. (2010) estimate that the load of all dissolved and particulate forms of C, N, and P in  
23 African river basins have increased in the period 1970 – 2000, and further increases are predicted for all dissolved fractions  
24 of N and P between 2000 – 2050, although C fractions and particulate forms of N and P are modelled to decrease. Predicted  
25 decreases of particulate loads are linked to the net effect of climate change and reservoir construction, which alter hydrology,  
26 nutrient retention and sediment carrying capacity of rivers (Yasin et al., 2010), and which store ~25% of annual sediment  
27 load carried over the African landmass (Syvitski et al., 2005), while the increasing dissolved nutrient loads are related to the  
28 rising population, as well as increased per capita gross domestic product (GDP) and meat consumption, with these factors  
29 driving up the terrestrial inputs of manure, fertiliser and sewage derived N and P (Yasin et al., 2010).

30 British settlement brought European land-use practises to the Kenyan highlands early in the 20th century, triggering severe  
31 soil erosion in, and elevated sediment fluxes from, the Athi-Galana-Sabaki (A-G-S) River basin (Champion, 1933; Fleitmann  
32 et al. 2007). These terrigenous sediments have had a significant impact on the environment surrounding the outflow of the  
33 Sabaki River in the Indian Ocean, for example, by increasing coral stress (van Katwijk et al., 1993) and spreading seagrass  
34 beds on local reef complexes, as well as siltation and infilling of the Sabaki estuary and the rapid progradation of nearby



1 shorelines (Giesen and van de Kerkhof, 1984). In order to alleviate regional water scarcity, construction of reservoirs on the  
2 Athi River have been under consideration for decades, the implementation of which could modify the magnitude of sediment  
3 delivery to the coastal zone (van Katwijk et al., 1993) as previously observed in the neighbouring Tana River (Finn, 1983;  
4 Tamooh et al., 2012).

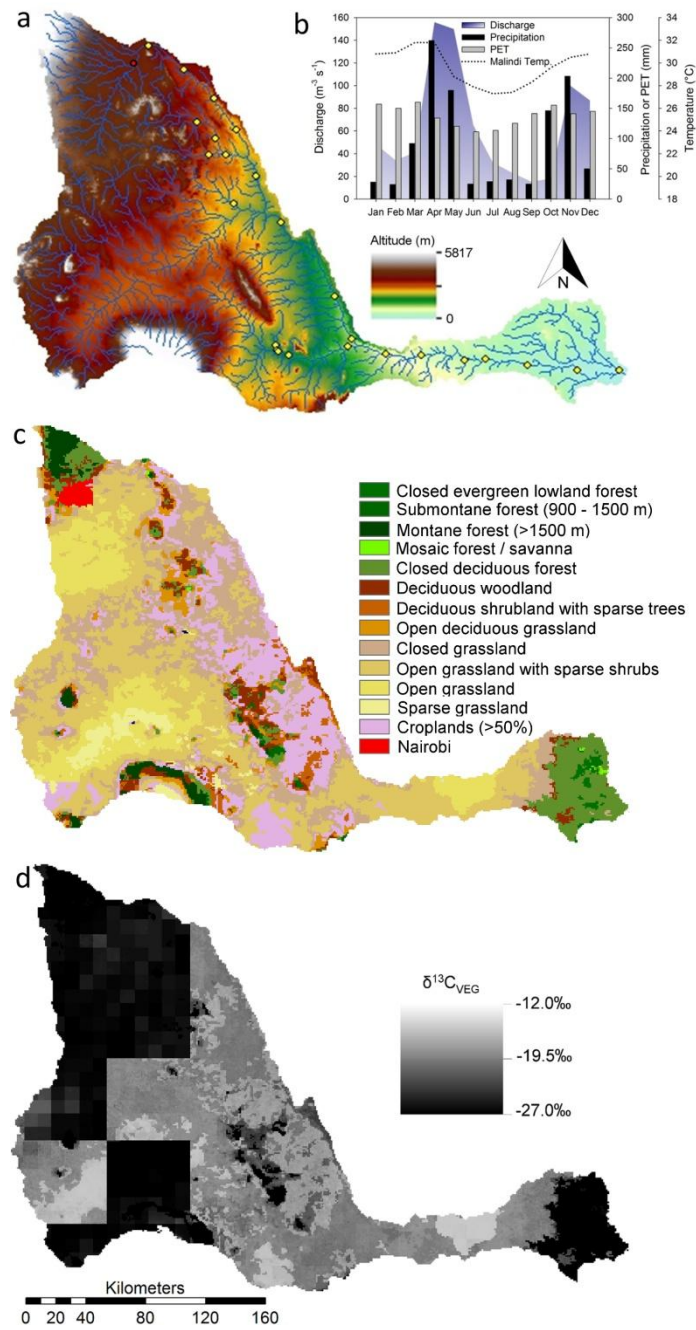
5 Here, we present a 2-year biogeochemical record at fortnightly resolution for the riverine end-member of the A-G-S system,  
6 and in light of the planned construction of the Thwake Multi-purpose Dam (currently awaiting tender approval, see  
7 <http://www.afdb.org/projects-and-operations/project-portfolio/project/p-ke-e00-008/>), we provide estimates for sediment and  
8 nutrient export rates from the A-G-S system whilst still under pre-dam conditions.

## 9 **2 Materials and methods**

### 10 **2.1 Study area**

11 The Athi-Galana-Sabaki River basin is the second largest drainage basin ( $\sim 46600 \text{ km}^2$ ) in Kenya. The headwaters are located  
12 in central and south-east Kenya, in the vicinity of Nairobi city (Fig. 1), draining agricultural areas (predominantly tea and  
13 coffee plantations) which provide the livelihood of 70% of the regional population (Kithia, 1997). Industrial activities and  
14 informal settlements dominate land-use around Nairobi, with livestock and small-scale irrigation activities also present  
15 downstream. The basin landcover is dominated by grasslands biomes ( $\sim 65\%$ ) rich in  $C_4$  species (Fig. 1), with agriculture  
16 accounting for  $\sim 15\%$  and the region of Nairobi  $< 1\%$ . Forest biomes dominated by  $C_3$  vegetation are isolated to higher  
17 altitude regions in the basin headwaters, as well as in the coastal region where the Sabaki River discharges to the Indian  
18 ocean at Malindi Bay (Fig. 1).

19 Precipitation ranges between 800 and 1200  $\text{mm yr}^{-1}$  in the highly populated central highlands surrounding Nairobi, to 400–  
20 800  $\text{mm yr}^{-1}$  in the less populated, lower altitude, and semi-arid south-east of Kenya. Two dry seasons (January–February,  
21 hereafter JF; June–September, hereafter JJAS) intersperse a long (March–May, hereafter MAM) and short (October–  
22 December, hereafter OND) wet season. Only during the MAM and OND periods does monthly precipitation exceed potential  
23 evaporation-transpiration within the basin (Fig. 1), and accordingly the annual hydrograph displays bimodal discharge, with  
24 an average flow rate of  $49 \text{ m}^3 \text{ s}^{-1}$  between 1957–1979 (Fleitmann et al. 2007). Dry season flow rates as low as  $0.5 \text{ m}^3 \text{ s}^{-1}$   
25 compare to peak wet season flow rates of up to  $5000 \text{ m}^3 \text{ s}^{-1}$  (Delft Hydraulics, 1970; Fleitmann et al., 2007). Oscillations  
26 between El Niño and La Niña conditions have a strong influence on the decadal patterns of river discharge, where extended  
27 severe drought is broken by intense and destructive flooding (Mogaka et al., 2006). The pre-1960 sediment flux of  $0.06 \text{ Tg}$   
28  $\text{yr}^{-1}$  is dwarfed by modern day flux estimates of  $5.7$  and  $14.3 \text{ Tg yr}^{-1}$  (Van Katwijk et al., 1993; Kitheka, 2013), with the  
29 rapid increase in sediment flux over the preceding half-century attributed to a combination of intensified land use practices,  
30 the highly variable climatic conditions and extremely erosive native soils. More detailed information regarding basin settings  
31 may be found in Marwick et al. (2014a).



1  
2 **Figure 1.** The Athi-Galana-Sabaki River basin: (a) digital elevation model, (b) mean monthly variation of hydrological and climate  
3 parameters including discharge at the outlet (shaded area; data from 1959–1977), precipitation (black bar) (from Fleitmann et al.,  
4 2007), potential evapotranspiration (PET; grey box), and the maximum air temperature in Malindi (A-G-S outlet; dotted black  
5 line), (c) GLC2000 vegetation biomes (Mayaux et al., 2004), and (c) Crop corrected vegetation *isoscape* (extracted from Still and  
6 Powell (2010)). The yellow dots in (a) mark the site locations from Marwick et al. (2014a). Data presented here was collected at the  
7 most eastern sampling locality (site S20 from Marwick et al. (2014)), while our discharge estimates were calculated from data  
8 collected at the adjacent site directly west (site S19 from Marwick et al. (2014)).



## 1 2.2 Sampling and analytical techniques

2 Physico-chemical parameters and biogeochemistry of the Sabaki River were monitored bi-weekly (i.e. fortnightly)  
3 approximately 2 km upstream of Sabaki Bridge (approximately 5 km upstream of the river outlet to Malindi Bay) for the  
4 period October 2011 to December 2013. Water temperature, conductivity, dissolved oxygen ( $O_2$ ) and pH were measured in  
5 situ with a YSI ProPlus multimeter, whereby the  $O_2$  and pH probes were calibrated on each day of data collection using  
6 water saturated air and United States National Bureau of Standards buffer solutions (4 and 7), respectively. Samples for  
7 dissolved gases ( $CH_4$ ,  $N_2O$ ) and the stable isotope composition of dissolved inorganic C ( $\delta^{13}C_{DIC}$ ) were collected from mid-  
8 stream at ~0.5 m depth with a custom-made sampling bottle consisting of an inverted 1L polycarbonate bottle with the  
9 bottom removed, and ~0.5 m of tubing attached in the screw cap (Abril et al. 2007). 12 mL exetainer vials (for  $\delta^{13}C_{DIC}$ ) and  
10 50 mL serum bottles (for  $CH_4$  and  $N_2O$ ) were filled from water flowing from the outlet tubing, poisoned with  $HgCl_2$ , and  
11 capped without headspace. Approximately 2000 mL of water was collected 0.5 m below the water surface for other  
12 particulate and dissolved variables, and filtration and sample preservation was performed in the field within 2 h of sampling.  
13 Samples for total suspended matter (TSM) were obtained by filtering 60-250 mL of water on pre-combusted (4 h at 500°C)  
14 and pre-weighed glass fibre filters (47mm GF/F, 0.7  $\mu m$  nominal pore size), and dried in ambient air during the fieldwork.  
15 Samples for determination of particulate organic C (POC), particulate nitrogen (PN) and C isotope composition of POC  
16 ( $\delta^{13}C_{POC}$ ) were collected by filtering 40-60 mL of water on pre-combusted 25 mm GF/F filters (0.7  $\mu m$  nominal pore size).  
17 The filtrate from the TSM filtrations was further filtered on 0.2  $\mu m$  polyethersulfone syringe filters (Sartorius, 16532-Q) for  
18 total alkalinity (TA), DOC and  $\delta^{13}C_{DOC}$  (8-40 mL glass vials with Polytetrafluoroethylene coated septa). TA was analysed by  
19 automated electro-titration on 50 mL samples with 0.1 mol  $L^{-1}$  HCl as titrant (reproducibility estimated as typically better  
20 than  $\pm 3 \mu mol kg^{-1}$  based on replicate analyses).  
21 For the analysis of  $\delta^{13}C_{DIC}$ , a 2 ml helium (He) headspace was created, and  $H_3PO_4$  was added to convert all DIC species to  
22  $CO_2$ . After overnight equilibration, part of the headspace was injected into the He stream of an elemental analyser – isotope  
23 ratio mass spectrometer (EA-IRMS, ThermoFinnigan Flash HT and ThermoFinnigan DeltaV Advantage) for  $\delta^{13}C$   
24 measurements. The obtained  $\delta^{13}C$  data were corrected for the isotopic equilibration between gaseous and dissolved  $CO_2$  as  
25 described in Gillikin and Bouillon (2007), and measurements were calibrated with certified reference materials LSVEC and  
26 either NBS-19 or IAEA-CO-1. Concentrations of  $CH_4$  and  $N_2O$  were determined via the headspace equilibration technique  
27 (20 mL  $N_2$  headspace in 50 mL serum bottles) and measured by gas chromatography (GC, Weiss 1981) with flame  
28 ionization detection (GC-FID) and electron capture detection (GC-ECD) with a SRI 8610C GC-FID-ECD calibrated with  
29  $CH_4:CO_2:N_2O:N_2$  mixtures (Air Liquide Belgium) of 1, 10 and 30 ppm  $CH_4$  and of 0.2, 2.0 and 6.0 ppm  $N_2O$ , and using the  
30 solubility coefficients of Yamamoto et al. (1976) for  $CH_4$  and Weiss and Price (1980) for  $N_2O$ .  
31 25 mm filters for POC, PN and  $\delta^{13}C_{POC}$  were decarbonated with HCl fumes for 4 h, re-dried and packed in Ag cups. POC,  
32 PN, and  $\delta^{13}C_{POC}$  were determined on the abovementioned EA-IRMS using the thermal conductivity detector (TCD) signal of  
33 the EA to quantify POC and PN, and by monitoring m/z 44, 45, and 46 on the IRMS. An internally calibrated acetanilide and



1 sucrose (IAEA-C6) were used to calibrate the  $\delta^{13}\text{C}_{\text{POC}}$  data and quantify POC and PN, after taking filter blanks into account.  
2 Reproducibility of  $\delta^{13}\text{C}_{\text{POC}}$  measurements was better than  $\pm 0.2\text{‰}$ . Samples for DOC and  $\delta^{13}\text{C}_{\text{DOC}}$  were analysed either on a  
3 Thermo HiperTOC IRMS (Bouillon et al. 2006), or with an Aurora1030 TOC analyser (OI Analytical) coupled to a Delta V  
4 Advantage IRMS. Typical reproducibility observed in duplicate samples was in most cases  $<\pm 5\text{ \%}$  for DOC, and  $\pm 0.2\text{‰}$  for  
5  $\delta^{13}\text{C}_{\text{DOC}}$ .  
6 Our dataset for  $\text{CH}_4$  and  $\text{N}_2\text{O}$  has been used in a continental-scale data synthesis in Borges et al. (2015a), but are discussed  
7 here in more detail.

### 8 **2.3 Discharge estimates**

9 Historical discharge observations and daily gauge height data for the sampling period was provided by the Water Resource  
10 Management Authority (WRMA), Machakos, Kenya. Due to the poor resolution of discharge and gauge data at the Sabaki  
11 Bridge north of Malindi (gauge # 3HA06) over the monitoring period, the finer fidelity record from the Baricho station  
12 (gauge # 3HA13) was used, situated approximately 50 km upstream of our biogeochemical monitoring station (i.e. site S20  
13 from basin-wide sampling campaigns, see Marwick et al. 2014a). With discharge measurements from 2006 and 2007 ( $n =$   
14 11), care of WRMA, we developed a rating curve to calculate daily discharge from available gauge data (Fig. 2a). As seen in  
15 Fig. 2a, the limited and poor spread of discharge measurements results in extrapolation for gauge heights  $< 1\text{ m}$  and  $> 3\text{ m}$ .  
16 Although Kenyan rivers have been suggested to export up to 80% of annual sediment load during pulse discharge events  
17 over few days (Dunne, 1979), the timeframe of these event pulses is typically short-lived relative to more mundane flow  
18 conditions, and at heights for example  $< 3\text{ m}$  (which account for  $\sim 97\text{ \%}$  of gauge data) we have reasonable confidence that the  
19 rating curve reflects in-situ conditions. Given the general positive correlation between discharge and sediment concentration,  
20 and disregarding possible hysteresis in discharge-sediment flux dynamics (which have been shown for the neighbouring  
21 Tana River), we suspect the greatest error in our discharge estimates is when gauge height exceeds 3 m.  
22 The Baricho gauge height dataset contains a 2 month period of no measurement (1<sup>st</sup> of February to 31<sup>st</sup> March, 2013). For  
23 this period, the daily discharge was estimated as the average discharge for that day over the previous 10 years (2003 – 2012).

### 24 **2.4 Suspended sediment and C, N, and P flux estimates**

25 Annual flux estimates for suspended sediments and the various riverine fractions of particulate and dissolved C,  
26 N and P were calculated with the discharge data above. We interpolated linearly between the concentrations  
27 measured on consecutive sampling dates in order to establish concentrations for every day of the study period.  
28 The daily concentrations were then multiplied by daily discharge and summed over the study period to establish  
29 annual flux estimates.



## 1 **3 Results**

### 2 **3.1 Discharge**

3 All data (excluding results for  $\text{NH}_4^+$ ,  $\text{NO}_3^-$  and  $\text{PO}_4^{3-}$ ) are presented for the period between October 2011 and  
4 September 2013, encompassing two full seasons each of short wet (Oct. – Dec.; OND), short dry (Jan. – Feb.;  
5 JF), long wet (Mar. – May; MAM) and long dry (Jun. – Sep.; JJAS). Over the monitoring period, daily discharge  
6 (Fig. 2b; see also Supplementary Materials, Table 1) varied between  $13 \text{ m}^3 \text{ s}^{-1}$  and  $2032 \text{ m}^3 \text{ s}^{-1}$ , with mean and  
7 median flow rates of  $139 \text{ m}^3 \text{ s}^{-1}$  and  $51 \text{ m}^3 \text{ s}^{-1}$ , respectively, compared to the average flow rate of  $73 \text{ m}^3 \text{ s}^{-1}$   
8 reported by Kitheka (2013) for 2001 – 2003 and noted as a relatively wet period. The average annual discharge  
9 throughout the monitoring period totalled  $\sim 4.4 \text{ km}^3$ , considerably less than the  $\sim 10.7 \text{ km}^3$  used by Mayorga et al.  
10 (2010) and approximately double that reported by Kitheka (2013) ( $\sim 2.3 \text{ km}^3$ ) for the period 2001 – 2003. There  
11 was negligible inter-annual variation of total discharge for the monitoring period. Discharge during the wet  
12 seasons (MAM + OND) accounted for 82% and 79% of annual discharge for 2011 – 2012 and 2012 – 2013,  
13 respectively, while 59% and 51% of annual discharge occurred during the upper 10% of daily flows for the same  
14 periods.

15 Sampling of  $\text{NH}_4^+$ ,  $\text{NO}_3^-$  and  $\text{PO}_4^{3-}$  was conducted over a different timeframe to the rest of the data presented  
16 here. The range in daily discharge over this time period (21<sup>st</sup> Dec. 2012 to 20<sup>th</sup> Dec. 2013) reflects the ranges  
17 reported above, although the mean flow rate was somewhat elevated ( $169 \text{ m}^3 \text{ s}^{-1}$ ). Total annual discharge was  $5.3 \text{ km}^3$ , with between 83% of total annual discharge occurring during the wet seasons.

18 Throughout the Results and Discussion we use discharge values of  $\leq 68 \text{ m}^3 \text{ s}^{-1}$  and  $\geq 152 \text{ m}^3 \text{ s}^{-1}$  when referring to  
19 low and high flow (hereafter LF and HF) conditions respectively, corresponding to the maximum value for the  
20 upper 80% of daily dry season flows and minimum value for the upper 30% of daily wet season flows.

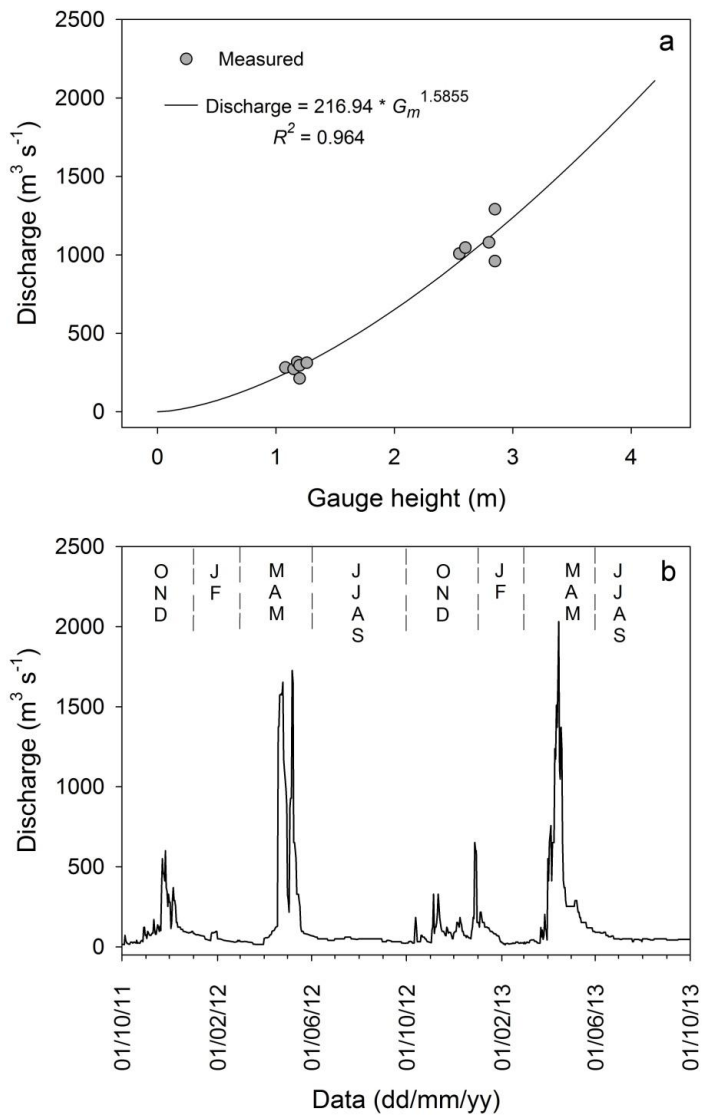
### 22 **3.2 Physico-chemical parameters**

23 Water temperature varied from  $24.1^\circ\text{C}$  to  $33.9^\circ\text{C}$  (average  $\pm 1 \text{ SD} = 29.8 \pm 2.0^\circ\text{C}$ ), with considerable variability intra- and  
24 inter-seasonally. The coolest temperatures occurred at the end of the MAM wet season and during the JJAS dry season. pH  
25 varied widely across the sampling period (range = 4.6 to 10.1) yet maintained an average of  $7.1 \pm 1.1$ . Most basic conditions  
26 were typically observed during lower flow periods of the dry seasons. %O<sub>2</sub> saturation ranged between 23.3% and 130.0%,  
27 with least saturated conditions observed during the JJAS dry season of 2013. There was no clear relationship between  
28 discharge and conductivity, with the latter's range varying sporadically over the sampling period from  $113.0 \mu\text{S cm}^{-1}$  to  
29  $1080.0 \mu\text{S cm}^{-1}$  (average =  $487.1 \pm 254.5 \mu\text{S cm}^{-1}$ ). Total alkalinity (TA) varied over an order of magnitude (0.475 to 4.964  
30 mmol kg<sup>-1</sup>) with an average of  $2.438 \pm 0.872 \text{ mmol kg}^{-1}$ . There was poor correlation between discharge and TA, with



1 observed peaks scattered across the hydrograph, suggesting a simple two source scenario of baseflow and high flow dilution  
2 is inadequate to explain the seasonal variability for the A-G-S system. All data for physico-chemical parameters and those  
3 outlined below are presented in Table 1 of the Supplementary Materials.

4



5  
6 Figure 2. (a) Discharge rating curve for the Sabaki River at the Baricho gauge station (3HA13). (b) Calculated daily discharge for  
7 the two year monitoring period. Note, one anomalous gauge reading on the 12/11/2012 provides an upper discharge estimate of  
8  $41332 \text{ m}^3 \text{s}^{-1}$ , over a magnitude larger than the next highest daily discharge estimate ( $3441 \text{ m}^3 \text{s}^{-1}$ ). Given the discharge estimates  
9 on the preceding (11/11/2012) and following days (13/11/2012) were  $312$  and  $218 \text{ m}^3 \text{s}^{-1}$ , respectively, and also reported historical  
10 maximum daily discharge of  $\sim 5000 \text{ m}^3 \text{s}^{-1}$  (Delft Hydraulics, 1970), we linearly interpolated the gauge data for the 12/11/2012 from  
11 the values of adjacent days thereby lowering the discharge estimate for this date to  $249 \text{ m}^3 \text{s}^{-1}$ . The curve in (a) was developed  
12 from the limited dataset ( $n = 11$ ) of recent discharge measurements (2006 – 2007; grey circles) on the Sabaki River at Baricho.  
13 (data supplied by WRMA, Machakos)



### 1 3.3 Bulk concentrations

2 The concentrations of TSM, POC, particulate N (PN) and total particulate phosphorus (TPP) are shown in Fig. 3, as well as  
3 the stable isotope composition of POC and PN, with most variables showing complex variation across the hydrological year.  
4 The Sabaki River exported TSM varying in concentration from 50.0 to 3796.7 mg L<sup>-1</sup> (Fig. 3a), containing POC at  
5 concentrations between 3.5 and 74.6 mg L<sup>-1</sup> (Fig. 3b). The lower and upper TSM and POC concentrations were associated  
6 with the JJAS (dry) and OND (wet) periods of 2011 respectively. The contribution of POC to the TSM pool (hereafter,  
7 %POC) indicates a wide bi-annual variation in suspended sediment load from OC-poor (0.3%) to OC-rich (14.9%), with the  
8 highest %POC occurring when discharge is < 100 m<sup>3</sup> s<sup>-1</sup> (Fig. 4a) and at lower TSM concentrations (Fig. 4b). The large  
9 range for the C stable isotope ( $\delta^{13}\text{C}$ ) of the POC pool ( $\delta^{13}\text{C}_{\text{POC}}$ ; -23.3‰ to -14.5‰) displayed complex temporal patterns  
10 with no obvious trends across seasons nor with discharge (Fig. 3b). Particulate N ranged in concentration from 0.3 to 9.4 mg  
11 L<sup>-1</sup> (Fig. 3c), while the ratio of POC to PN (as a weight:weight ratio; hereafter, POC:PN) varied from 6.6 to 17.4, with an  
12 average value of  $9.4 \pm 1.7$  ( $n = 42$ ). The N stable isotope composition ( $\delta^{15}\text{N}$ ) of PN ( $\delta^{15}\text{N}_{\text{PN}}$ ) showed considerable fluctuation  
13 (from -3.1 to +15.9‰; Fig. 3c), with the most <sup>15</sup>N-enriched PN recorded at the beginning of the OND period of 2011 –  
14 2012 and during the JJAS period of 2012 – 2013. The TPP load showed complex temporal variability (Fig. 3d), with  
15 concentrations ranging between 61.2 and 256.1 µg L<sup>-1</sup> and displayed negligible correlation with discharge. Although TPP  
16 generally rose during (or slightly preceding) peak discharge, the highest values were recorded under LF conditions during  
17 the 2012 – 2013 JJAS period.  
18 The dissolved organic C (DOC) concentration fluctuated from 3.3 to 9.3 mg L<sup>-1</sup> (Fig. 5a), with lowest and highest  
19 concentrations observed during the JJAS and MAM periods of 2013, respectively. The highest DOC concentrations were  
20 regularly observed in the weeks following wet season peak discharge. The contribution of DOC to the total OC (TOC) pool  
21 ranged between 15% and 68% (accounting for 20% and 32% of annual TOC export during 2011 – 2012 and 2012 – 2013  
22 respectively) with no clear seasonal trend. Akin to the  $\delta^{13}\text{C}_{\text{POC}}$ , the  $\delta^{13}\text{C}$  composition of the DOC pool ( $\delta^{13}\text{C}_{\text{DOC}}$ ) displayed  
23 complex variability over a large range (-29.3‰ to -17.9‰) with no obvious relationship with either seasonality or discharge  
24 (Fig. 5a). On average, the DOC was more depleted in <sup>13</sup>C than concurrent POC samples ( $\delta^{13}\text{C}_{\text{POC}} - \delta^{13}\text{C}_{\text{DOC}} = 2.8 \pm 2.9$ ‰,  $n = 40$ ).  
25 The  $\delta^{13}\text{C}$  composition of the DIC pool ( $\delta^{13}\text{C}_{\text{DIC}}$ ) shifted between -12.4‰ and -3.2‰ and also shows a complex pattern  
26 across the hydrograph (Fig. 5b), though the DIC pool was generally more enriched in <sup>13</sup>C during LF periods and more <sup>13</sup>C-  
27 depleted over the wet seasons.  
28 The concentration range for NH<sub>4</sub><sup>+</sup>, NO<sub>3</sub><sup>-</sup>, and PO<sub>4</sub><sup>3-</sup> over the 1-yr period were 7.1 to 309.6 µmol L<sup>-1</sup>, <0.1 to 506.9 µmol L<sup>-1</sup>,  
29 and 1.1 to 322.6 µmol L<sup>-1</sup> respectively (Fig. 6). No strong seasonal pattern is apparent in the dissolved inorganic N fractions  
30 (Figs. 6b and 6c), although peak concentrations generally occur at below average discharge conditions (i.e. when  $Q < 169$  m<sup>3</sup>  
31 s<sup>-1</sup> then the average ( $\pm 1$  SD) DIN concentration is  $172.2 \pm 140.1$  µmol L<sup>-1</sup> ( $n = 20$ ), whereas when  $Q \geq 169$  m<sup>3</sup> s<sup>-1</sup> then the  
32 average ( $\pm 1$  SD) DIN concentration is  $59.6 \pm 26.3$  µmol L<sup>-1</sup> ( $n = 5$ )). The concentration of PO<sub>4</sub><sup>3-</sup> displayed an erratic pattern  
33



1 over the course of the year (Fig. 6d). Concentrations were highly variable at below average flow conditions (i.e. when  $Q <$   
2  $169 \text{ m}^3 \text{ s}^{-1}$  the average ( $\pm 1 \text{ SD}$ )  $\text{PO}_4^{3-}$  concentration is  $105.7 \pm 97.2 \text{ } \mu\text{mol L}^{-1}$  ( $n = 20$ )), whereas concentrations became  
3 comparatively low during above average discharge (i.e. when  $Q \geq 169 \text{ m}^3 \text{ s}^{-1}$  then the average ( $\pm 1 \text{ SD}$ )  $\text{PO}_4^{3-}$  concentration  
4 is  $34.8 \pm 31.0 \text{ } \mu\text{mol L}^{-1}$  ( $n = 5$ )).

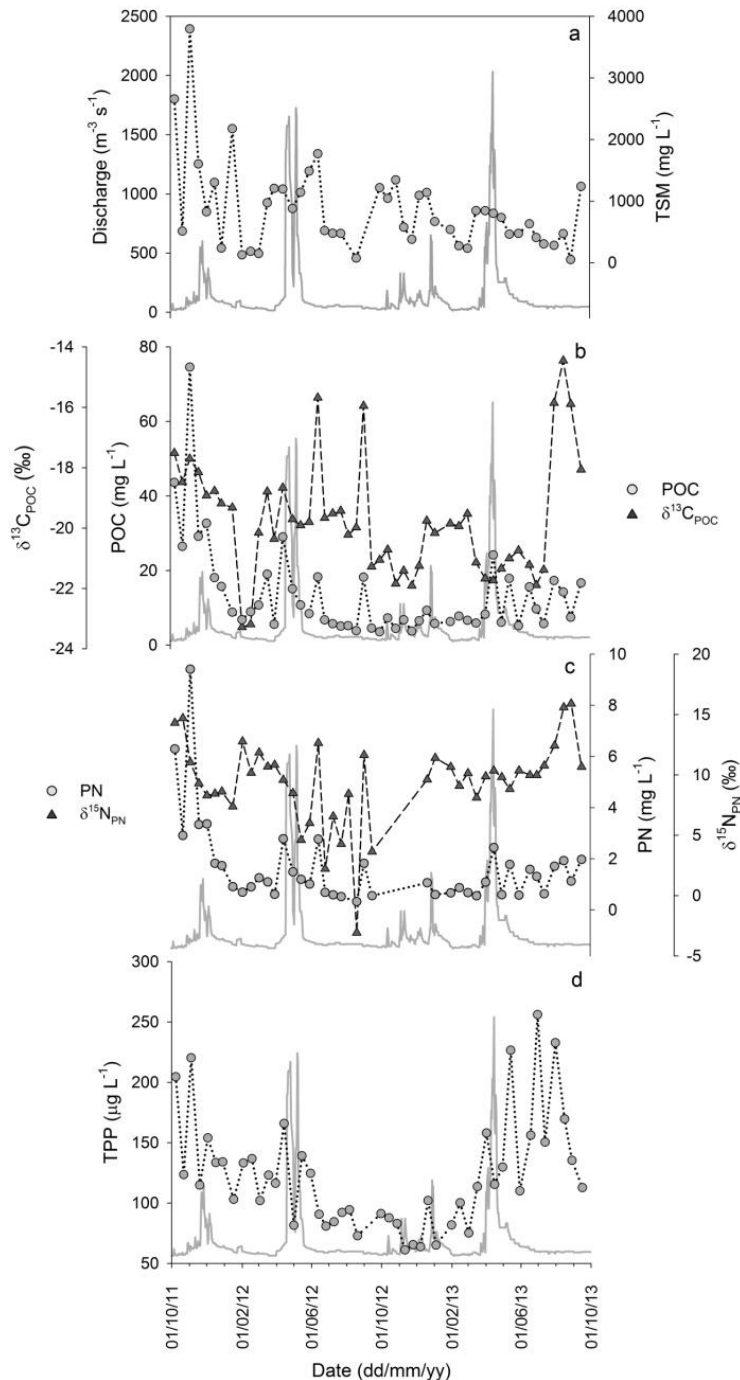
5 The river was consistently oversaturated in dissolved  $\text{CH}_4$  relative to the atmosphere (from 499% to 135,111%) with a  
6 concentration range between 10 and  $2,838 \text{ nmol L}^{-1}$  (Fig. 7a). Although  $\text{CH}_4$  peaks occurred in both dry and wet season, the  
7 largest annual peaks occur at the end of the JJAS dry period. Concentrations of dissolved  $\text{N}_2\text{O}$  (Fig. 7b) varied from 5.9 and  
8  $26.6 \text{ nmol L}^{-1}$ , corresponding to oversaturation of 100% to 463% relative to atmospheric concentrations.  $\text{N}_2\text{O}$  concentrations  
9 were highest during the OND period of 2011 – 2012, and otherwise showed maximum concentrations preceding peak  
10 discharge during the MAM period of each year.

### 11 **3.4 Annual flux and yield of particulate and dissolved fractions**

12 Annual material flux estimates to the coastal zone for TSM and various C, N, and P fractions are provided in Table 1.  
13 Briefly, our data suggest a mean flux of  $4.0 \text{ Tg yr}^{-1}$ ,  $70.6 \text{ Gg C yr}^{-1}$  and  $24.1 \text{ Gg C yr}^{-1}$  for TSM, POC and DOC  
14 respectively, corresponding to mean annual %POC of 1.8%, and mean annual contribution of DOC to the TOC pool  
15 (hereafter %DOC) of 26%. Bi-annually, wet season (OND, MAM) flows carried >80% of the total load for TSM (~86%),  
16 POC (~89%) and DOC (~81%), with the MAM period accounting for > 50% of TSM, POC and DOC annual export.  
17 Estimates of mean annual flux of PN and TPP were  $7.5 \text{ Gg}$  and  $0.5 \text{ Gg}$  respectively, and > 80% of bi-annual export of PN  
18 (~89%) and TPP (~82%) occurred during the wet seasons, with > 50% of the annual flux occurring over the MAM period.  
19 Annual dissolved nutrient flux estimates (Table 1) were  $2.3 \text{ Gg}$ ,  $4.3 \text{ Gg}$  and  $11.2 \text{ Gg}$  for  $\text{NH}_4^+$ ,  $\text{NO}_3^-$  and  $\text{PO}_4^{3-}$  respectively.  
20 Approximately 75% of  $\text{NH}_4^+$  export occurred during the wet seasons, whereas only 66% of  $\text{NO}_3^-$  export occurred over the  
21 same period. Approximately 79% of annual  $\text{PO}_4^{3-}$  export took place during the wet seasons, with a greater proportion  
22 exported over the OND wet season (45%) than the MAM wet season.

23 Various surface area estimates are reported for the A-G-S basin, ranging from  $40000 \text{ km}^2$  (Giesen and van de Kerkhof, 1984;  
24 van Katwijk et al., 1993), to  $\sim 70000 \text{ km}^2$  (Fleitmann et al., 2007; Kitheka, 2013), and up to  $117000 \text{ km}^2$  by Mayorga et al.  
25 (2010). Using ArcGIS 10.1 and the river basins of Africa output of Lehner et al. (2006) (<http://hydrosheds.cr.usgs.gov>), we  
26 estimate the A-G-S basin covers an area of  $\sim 46750 \text{ km}^2$ .

27 Taking the above basin area estimate and the flux values detailed above, we estimate mean annual yields of  $84.6 \text{ Mg km}^{-2}$ ,  
28  $1.51 \text{ Mg C km}^{-2}$  and  $0.52 \text{ Mg C km}^{-2}$  for TSM, POC and DOC respectively (Table 1). Conservative mean annual yields for  
29 PN and TPP were  $161 \text{ kg N km}^{-2}$  and  $11 \text{ kg P km}^{-2}$ , while those of the dissolved fractions over the single hydrological year  
30 were  $49 \text{ kg N km}^{-2}$ ,  $93 \text{ kg N km}^{-2}$  and  $239 \text{ kg P km}^{-2}$  for  $\text{NH}_4^+$ ,  $\text{NO}_3^-$  and  $\text{PO}_4^{3-}$ , respectively (see also Supplementary  
31 Material, Table 2).

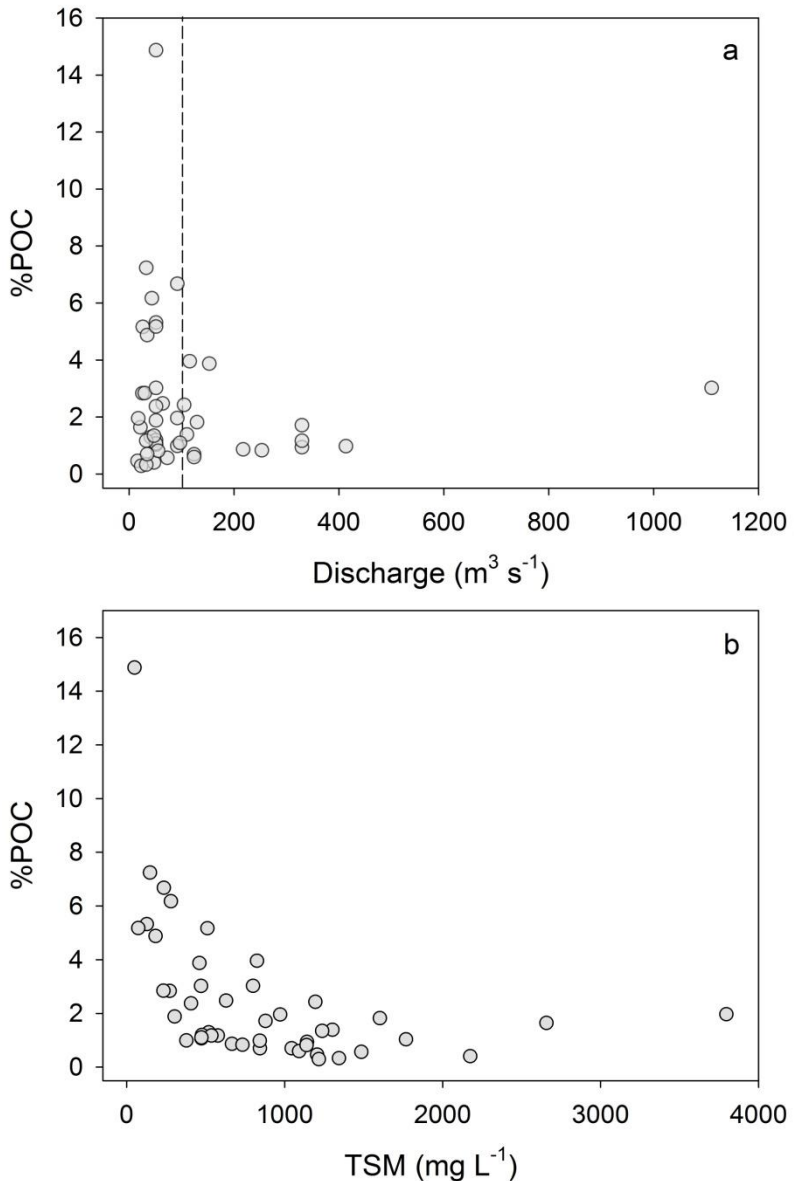


1

2 **Figure 3.** Discharge (solid grey line) and two years of monitoring the (a) total suspended matter concentration, the concentration  
 3 and stable isotope signature of (b) particulate organic carbon and (c) particulate nitrogen, and the concentration of (d) total  
 4 particulate phosphorus in the Sabaki River. In all figures grey circles represent bulk concentrations and dark triangles represent  
 5 stable isotope signatures.

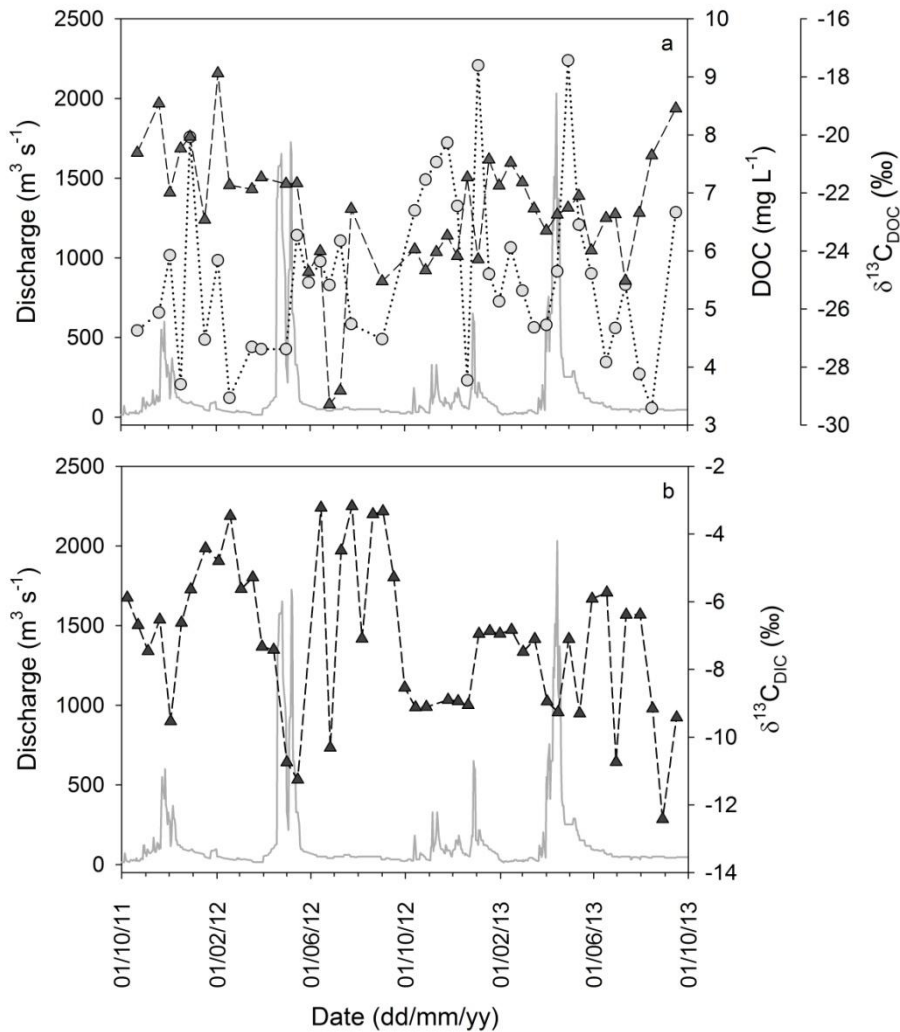


1



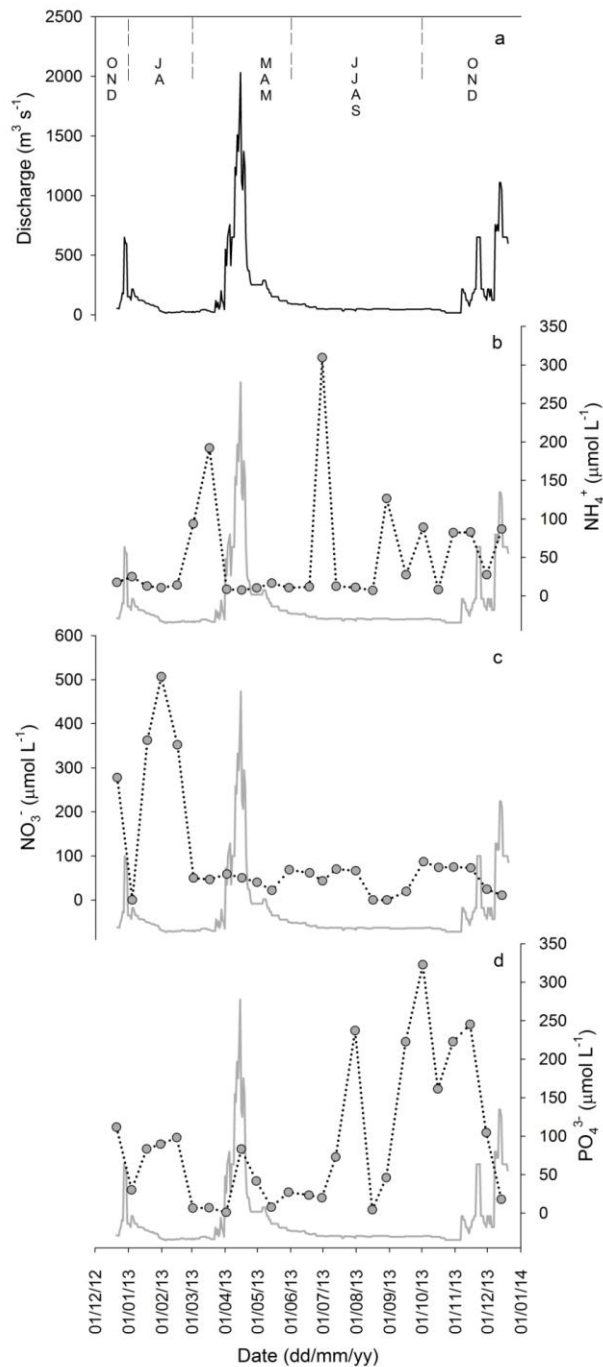
2

3 **Figure 4.** The relationship between the % contribution of particulate organic carbon to the total suspended load and (a) discharge,  
4 and (b) total suspended matter. The dashed line in (a) marks discharge of  $100 \text{ m}^3 \text{s}^{-1}$ , as cited in-text.



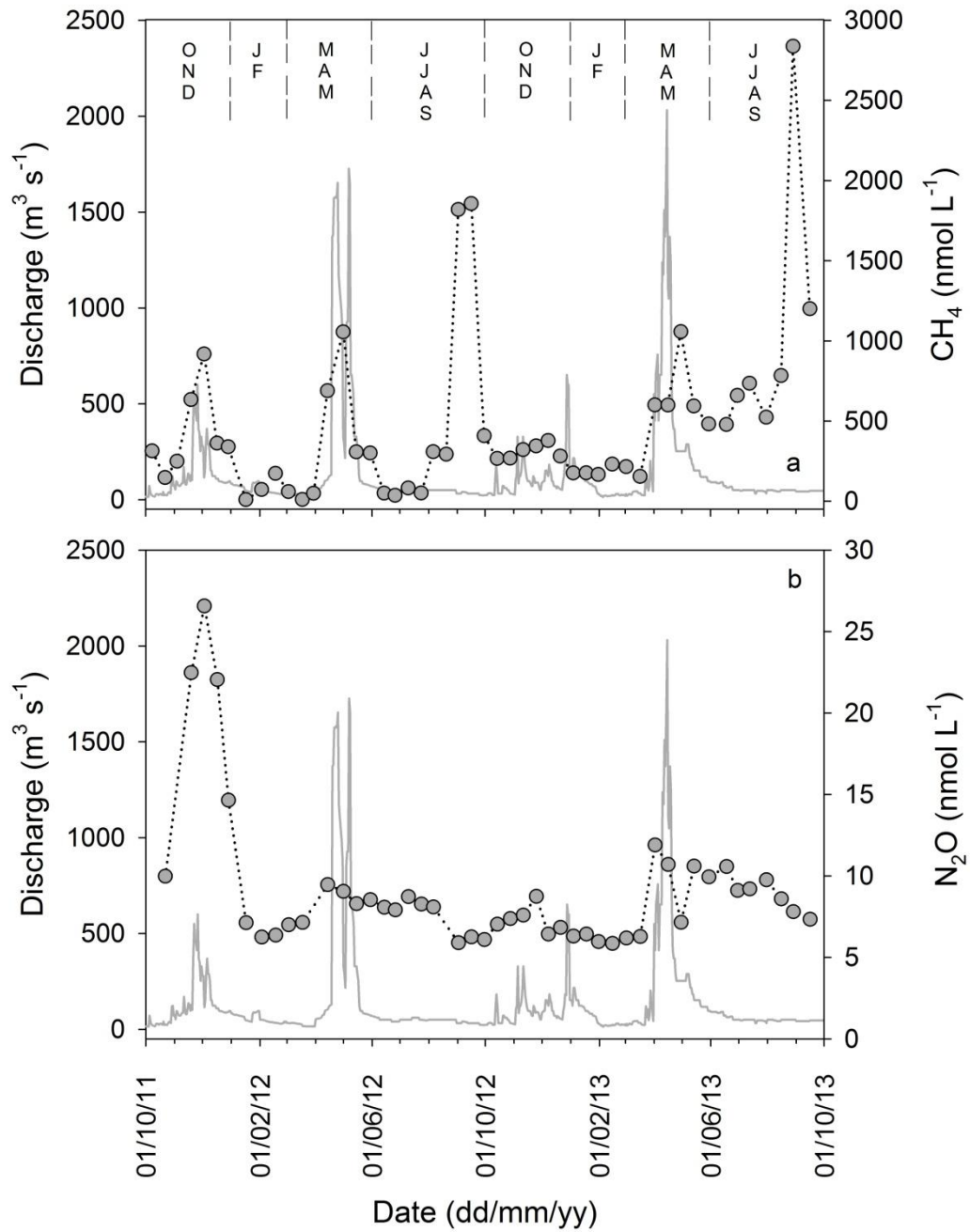
1

2 **Figure 5.** Discharge and two years of monitoring the dissolved (a) organic carbon concentration and carbon stable isotope  
3 signature, and (b) the carbon stable isotope signature of dissolved inorganic carbon in the Sabaki River. Grey circles represent  
4 bulk concentrations, with dark triangles for all stable isotope signatures.



1

2 **Figure 6. (a) Daily discharge rates and one year of monitoring the concentration of dissolved (b) ammonium, (c) nitrate and (d)**  
3 **phosphate in the Sabaki River. In figures (b) – (d) grey circles represent bulk concentrations.**



1  
2 **Figure 7.** Two years of monitoring concentrations of dissolved (a) methane and (b) nitrous oxide. Grey circles represent riverine  
3 gas concentrations.

4

5



1 **Table 1. Summary of annual fluxes, element ratios, and annual yields for the Athi-Galana-Sabaki basin from data reported here**  
 2 and from the NEWS2 export model (see Mayorga et al., 2010), as well as data for 2012 and 2013 from the neighbouring Tana  
 3 River basin at Garsen (Geeraert et al., in review).

	A-G-S	A-G-S (NEWS2)	Tana
<i>Flux</i>			
Basin area (km <sup>2</sup> )	46750	117230	81700
Discharge (km <sup>3</sup> yr <sup>-1</sup> )	4.39 <sup>a</sup>	10.75	4.32 - 4.71
Discharge (km <sup>3</sup> yr <sup>-1</sup> )	5.32 <sup>b</sup>		
TSM	4.0	38.8	4.1 - 4.9
POC	70.6	205.3	113 - 157
DOC	24.1	49.5	11 - 14
PN	9.4	16.4	
TPP	0.5	9.6	
DIN	6.6	7.4	
PO <sub>4</sub> <sup>3-</sup>	11.2	0.9	
%POC (of TSM)	1.8	0.5	
POC:PN	8.7	12.5	
%DOC (of TOC)	25.5	23.0	
<i>Yield</i>			
TSM	84.6	330.7	50.2 - 60.0
POC	1.51	1.75	1.38 - 1.92
DOC	0.52	0.42	0.13 - 0.17
PN	161	140	
TPP	11	82	
DIN	142	63	
PO <sub>4</sub> <sup>3-</sup>	239	8	

4  
 5 <sup>a</sup> All fractions except dissolved N and P: hydrological years 1<sup>st</sup> October 2011 to 30<sup>th</sup> September  
 6 2012 and 1<sup>st</sup> October 2012 to 30<sup>th</sup> September 2013.  
 7 <sup>b</sup> Dissolved N and P only: hydrological year 21<sup>st</sup> December 2012 to 14<sup>th</sup> December 2013.

## 8 **4 Discussion**

9 Although previous studies provide estimates of annual suspended sediment fluxes at the Sabaki outlet as well as annual yield  
 10 estimates for the A-G-S basin (Watermeyer, 1981; Munyao et al., 2003; Kitheka, 2013), their primary research focus lay  
 11 elsewhere, and none provide the comprehensive biogeochemical record at a comparable temporal scale as presented here.  
 12 The following discussion revolves around the main objectives of our study, including: (i) the quantification of annual



1 suspended matter, C, N and P fluxes and sediment yield, (ii) characterising the sources of particulate and dissolved fractions  
2 of C and N, and (iii) to provide indications to the water-atmosphere transfer of important greenhouse gases ( $\text{CH}_4$  and  $\text{N}_2\text{O}$ ) at  
3 the outlet of the Sabaki River. We conclude with consideration of the future anthropogenic impacts in the A-G-S basin and  
4 the consequences for material fluxes from the Sabaki River to the coastal zone.

#### 5 **4.1 Material fluxes, annual yields and their origin**

6 To the best of our knowledge, and excluding suspended matter, the estimates provided in Table 1 are the first quantifications  
7 of material fluxes from the A-G-S system. A suspended sediment flux of  $\sim 7.5$  to  $14.3 \text{ Tg yr}^{-1}$  is commonly cited for the A-  
8 G-S system (Watermeyer et al., 1981; van Katwijk et al., 1993; Fleitmann et al., 2007), which is approximately 2- to 3.5-fold  
9 greater than our conservative TSM flux estimate of  $\sim 4.0 \text{ Tg yr}^{-1}$ . A more recent estimate from Kitheka (2013) for the period  
10 2001 – 2003 ( $5.7 \text{ Tg yr}^{-1}$ ) is still greater than, though more comparable to, our own estimate above. Whereas we employed  
11 year-round bi-weekly monitoring and extrapolated fluxes from daily gauge height readings, Kitheka (2013) measured  
12 concurrent discharge and suspended matter concentrations at monthly to bi-weekly periodicity. The relative coarseness of  
13 sampling interval employed by Kitheka (2013), in combination with their acknowledgement that peak sediment flux often  
14 occurs prior to peak discharge i.e. sediment exhaustion effect (Rovira and Batalla, 2006; Oeurng et al., 2011; Tamooh et al.,  
15 2014), may pre-empt accurate extrapolation of the annual sediment flux from their limited dataset. For example, in order to  
16 accurately estimate fluxes in systems with an irregular hydrograph, such as the neighbouring Tana River (which experiences  
17 similar climatic conditions and annual hydrograph pattern to the A-G-S basin), monitoring at a recurrence interval of  $< 7$   
18 days has been recommended (Tamooh et al., 2014), also implying that the flux estimates presented here may be improved  
19 with a more refined sampling frequency.

20 If we normalise the basin area of  $\sim 70000 \text{ km}^2$  reported by Fleitmann et al. (2007) and Kitheka (2013) to the value reported  
21 here ( $\sim 46750 \text{ km}^2$ ), and subsequently recalculate their SY from their riverine sediment flux values, we find our SY of  $\sim 85$   
22  $\text{Mg km}^{-2} \text{ yr}^{-1}$  is considerably lower than the  $160$  to  $306 \text{ Mg km}^{-2} \text{ yr}^{-1}$  recalculated from Fleitmann et al. (2007) and the  $122$   
23  $\text{Mg km}^{-2} \text{ yr}^{-1}$  from Kitheka (2013).

24 Some have reported that prior to 1960 the suspended sediment load of the A-G-S basin was  $\sim 58 \text{ Gg yr}^{-1}$  (Watermeyer et al.,  
25 1981; Van Katwijk et al., 1993), which is equivalent to a SY of  $\sim 1 \text{ Mg km}^{-2} \text{ yr}^{-1}$ . Although indeed the A-G-S basin has been  
26 disturbed by anthropogenic practises since European arrival, this value needs to be met with some scepticism, as it represents  
27 an approximately 85-fold increase in annual soil loss over the preceding 50 years. In the neighbouring Tana River basin,  
28 Tamooh et al. (2014) estimated annual suspended sediment yields between  $46$  and  $48 \text{ Mg km}^{-2}$  at  $\sim 150 \text{ km}$  from the river  
29 mouth (basin area of  $66500 \text{ km}^2$ ). More recently, higher resolution dataset of Geeraert et al. (in review; see Table 1) for the  
30 Tana River at Garsen ( $\sim 70 \text{ km}$  from the river mouth, basin area of  $81700 \text{ km}^2$ ) estimated a suspended SY of  $50$  –  $60 \text{ Mg}$   
31  $\text{km}^{-2}$ , indicating that the relatively smaller A-G-S basin exports a comparable quantity of sediment annually to the coastal  
32 zone as that discharged from the much larger (and heavily regulated) Tana River basin.



1 The SY reported here is low compared to the global average of  $190 \text{ Mg km}^{-2} \text{ yr}^{-1}$  (Milliman and Farnsworth, 2011) and  
2 considerably less than the average of  $634 \text{ Mg km}^{-2} \text{ yr}^{-1}$  for the African continent recently reported by Vanmaercke et al.  
3 (2014). This may be somewhat surprising given the typically concentrated suspended sediment loads observed over the  
4 monitoring period (mean ( $\pm 1 \text{ SD}$ ) =  $865 \pm 712 \text{ mg L}^{-1}$ ; median =  $700 \text{ mg L}^{-1}$ ), but can be explained by the fact all TSM  
5 concentrations  $> 1500 \text{ mg L}^{-1}$  were observed at below HF discharge rates (i.e.  $< 152 \text{ m}^{-3} \text{ s}^{-1}$ ; see Fig. 3a). All the same, our  
6 SY estimate is over 3-fold greater than the average pre-dam SY of  $25 \text{ Mg km}^{-2} \text{ yr}^{-1}$  from the Congo, Nile, Niger, Zambezi  
7 and Orange rivers (draining  $> 40\%$  of the African landmass) (Milliman and Farnsworth, 2011). Sediment yield estimates  
8 from other arid tropical basins of Africa (e.g. Gambia, Limpopo, Niger, and Senegal rivers) are significantly lower (between  
9 3 to  $18 \text{ Mg km}^{-2} \text{ yr}^{-1}$ ; Milliman and Farnsworth, 2011), although reported yields of  $94 \text{ Mg km}^{-2} \text{ yr}^{-1}$  from the Rufiji  
10 (Tanzania) and  $88 \text{ Mg km}^{-2} \text{ yr}^{-1}$  from the Ayensu (Ghana), both arid tropical basins, are equivalent to what was observed in  
11 the A-G-S basin.

12 The annual POC yield ( $1.5 \text{ Mg C km}^{-2}$ ) from the A-G-S basin is equivalent to the global average of  $1.6 \text{ Mg C km}^{-2}$  (Ludwig  
13 et al., 1996), though almost triple the estimate of  $0.6 \text{ Mg C km}^{-2}$  by Tamooch et al. (2014) at their most downstream site on  
14 the neighbouring Tana River, and over seven-fold greater than the  $0.2 \text{ Mg C km}^{-2}$  reported from the largely pristine, wooded  
15 savannah dominated Oubangui River (Bouillon et al., 2014), the 2<sup>nd</sup> largest tributary to the Congo River. The over-riding  
16 influence of sewage inputs on the biogeochemistry of the A-G-S basin has been previously brought to attention by Marwick  
17 et al. (2014a), partially through investigation of the  $\delta^{15}\text{N}$  composition of the PN pool. The average  $\delta^{15}\text{N}_{\text{PN}}$  recorded across the  
18 monitoring period here was  $9.5 \pm 3.5\text{\textperthousand}$  ( $n = 43$ ), which sits above the 75<sup>th</sup> percentile of measurements within other African  
19 basins (see Marwick et al. (2014a), Fig. 10 therein), and reflects the range of  $\delta^{15}\text{N}$  signatures of  $\text{NH}_4^+$  (+7‰ to +12‰; Sebilo  
20 et al., 2006) and  $\text{NO}_3^-$  (+8‰ to +22‰; Aravena et al., 1993; Widory et al., 2005) sourced from raw waste discharge. As  
21 highlighted earlier, around 50% percent of Nairobi's population of 3 million live in slums with inadequate waste  
22 management facilities which leads to increasing water quality issues (Dafe, 2009; Kithiia and Wambua, 2010), providing an  
23 evident explanation for the POC-loaded sediment flux from the A-G-S basin in comparison to other African river basins.

24 The annual DOC yield from the A-G-S basin ( $0.5 \text{ Mg C km}^{-2}$ ) is markedly lower than the global mean of  $1.9 \text{ Mg C km}^{-2}$   
25 (Ludwig et al., 1996). The DOC yield is within the range of  $0.1$  to  $0.6 \text{ Mg C km}^{-2}$  reported for the Tana River (Tamooch et  
26 al., 2014), consistent with the global observation of low DOC concentrations in rivers of semi-arid regions (Spitz and  
27 Leenheer, 1991), and also falls between observations in tropical savannah basins of  $\sim 0.3 \text{ Mg C km}^{-2}$  for the Gambia River  
28 (Lesack et al., 1984) and  $\sim 0.9 \text{ Mg C km}^{-2}$  for the Paraguay River (Hamilton et al., 1997). Tamooch et al. (2014) attributed the  
29 low DOC yield in the Tana basin to low soil OC content (average of  $3.5 \pm 3.9\%$  OC) as well as high temperatures in the  
30 lower basin (Tamooch et al., 2012 and 2014). Surface soils (0 – 5 cm) in the A-G-S basin were of low OC content also,  
31 ranging between 0.4 to 8.9% OC with an average value of  $2.0 \pm 1.9\%$  ( $n = 19$ ; own unpublished data), although due to site  
32 selection, samples were not gathered from the relatively OC-rich soils of the upper A-G-S basin (see  
33 <http://www.ciesin.columbia.edu/afsis/mapclient/> and overlay 'Soil Organic Carbon Mean – Depth 0 – 5 cm').



1 In contrast to some other C<sub>4</sub>-rich tropical and sub-tropical river basins, the POC load in the Sabaki River (average  $\delta^{13}\text{C} =$   
2  $-19.7 \pm 1.9\text{\textperthousand}$ ) is marginally enriched in  $^{13}\text{C}$  compared to the basin-wide bulk vegetation  $\delta^{13}\text{C}$  value of  $-21.0\text{\textperthousand}$ , as estimated  
3 from the crop corrected vegetation *isoscape* of Africa in Still and Powell (2010) (Fig. 1c). For example, in the C<sub>4</sub>-dominated  
4 Betsiboka River basin of Madagascar, a consistent underrepresentation of C<sub>4</sub>-derived C in riverine OC pools was reported by  
5 Marwick et al. (2014b), with similar observations (particularly during dry season) within the Congo (Mariotti et al., 1991;  
6 Bouillon et al., 2012) and Amazon (Bird et al., 1992) basins and in rivers of Australia (Bird and Pousai, 1997) and Cameroon  
7 (Bird et al., 1994 and 1998), and is typically attributed to a greater portion of riverine OC sourced from the neighbouring C<sub>3</sub>-  
8 rich riparian zone relative to more remote C<sub>4</sub> dominated landscapes (i.e. grassland/savannah). Under this scenario, the C<sub>4</sub>-  
9 derived riverine OC component generally peaks during the wet season in response to the increased mobilisation of surface  
10 and sub-surface OC stocks from more distant C<sub>4</sub>-rich sources. At the outlet of the A-G-S basin, on the other hand, not only  
11 was POC more enriched in  $^{13}\text{C}$  (peak value of  $-14.5\text{\textperthousand}$ ) than values recorded in the neighbouring Tana basin ( $-19.5\text{\textperthousand}$ ;  
12 Tamooch et al. (2014)) or the C<sub>4</sub>-dominated Betsiboka basin ( $-16.2\text{\textperthousand}$ ; see Marwick et al. (2014b)), but these  $^{13}\text{C}$ -enriched  
13 POC loads occurred during consecutive JJAS periods (i.e. long dry season), and therefore, an alternative mechanism to the  
14 *riparian zone effect* outlined above is required to explain these dry season observations. One possibility is herbivore-  
15 mediated inputs of C<sub>4</sub>-derived OM to riverine OC pools, such as from livestock or large native African mammals, as has  
16 been reported for Lake Naivasha (Grey and Harper, 2002) and the Mara River in Kenya (Masese et al., 2015). The combined  
17 Tsavo West and Tsavo East National Parks, accounting for approximately 4% of the total surface area of Kenya, are  
18 dissected by the Galana River downstream of the confluence of the Tsavo with the Athi River. These national parks contain  
19 large populations of mammalian herbivores (Ngene et al., 2011), including elephants and buffalo (Supplementary Figure 1a  
20 and 1b, respectively), which graze on the C<sub>4</sub> savannah grasses and gravitate towards perennial water sources, such as the  
21 Galana River, during the dry season. More importantly, hippopotami (Supplementary Figure 1c) graze within the C<sub>4</sub>-rich  
22 savannas by night and excrete partially decomposed OM to the river during the day. Grey and Harper (2002) estimated the  
23 total quantity of excrement for the Lake Naivasha hippopotami population to be  $\sim 5.8 \text{ Gg yr}^{-1}$  ( $\sim 500$  individuals), assuming a  
24 consumption of 40 kg of biomass and a measured maximum wet weight of 8 kg of excrement on land per individual per  
25 night, with the remainder excreted to the lake during the day. This equates to approximately  $\sim 12 \text{ Mg yr}^{-1}$  per hippopotamus,  
26 and using the mean excrement compositions from Grey and Harper (2002) of 37% carbon and 1.5% nitrogen, results in  
27 hippopotamus-mediated delivery of  $\sim 740 \text{ kg C yr}^{-1}$  and  $\sim 30 \text{ kg N yr}^{-1}$ . To a lesser extent, additional terrestrial subsidies  
28 would be supplied by livestock using the river as a water source (Supplementary Figure 1d). Aerial census results from 2011  
29 identified  $\sim 80$  hippopotami within the combined Tsavo East (i.e. Athi and Galana rivers) and Tsavo West (i.e. Tsavo River)  
30 National Parks, considerably less than the  $\sim 4000$  reported from the Masai Mara National Reserve where the research of  
31 Masese et al. (2015) was conducted. Supplementary Figure 1 highlights the high density of other large mammals  
32 congregating around the Athi and Galana rivers, and though a smaller proportion of their total excrement will be released  
33 directly to the river relative to hippopotami, the combined quantity may be a significant contribution to the riverine OC pool  
34 under low flow conditions. Hence, it is reasonable to assume these herbivores deliver significant quantities of C<sub>4</sub>-derived



1 OM to inland waterways, especially during the dry season when other local water sources are depleted, with this being a time  
2 when the inputs may be particularly noticeable in riverine  $\delta^{13}\text{C}_{\text{POC}}$  signatures, as the contribution from other allochthonous  
3 sources would be minimised (especially  $\text{C}_4$ -derived OM, see Marwick et al. (2014b)) due to lower terrestrial runoff rates.  
4 The correlation between minor peaks in bulk POC and  $^{13}\text{C}$  enriched  $\delta^{13}\text{C}_{\text{POC}}$  signatures during the JJAS period of 2012  
5 supports this suggestion, when without a simultaneous increase in discharge, a short pulse of  $\text{C}_4$ -derived OC is observed in  
6 the Sabaki River.

7 The findings from the basin-wide campaigns reported in Marwick et al. (2014a) led to the suggestion that the concentration  
8 of DIN in export from the A-G-S basin likely peaks during the wet season, due to the significant processing and removal of  
9 DIN in the upper- to mid-basin during the dry season and which resulted in significantly lower DIN concentration at the  
10 monitoring station (i.e. site S20 from Marwick et al. (2014a)) relative to wet season observations. Our higher-resolution  
11 dataset, however, suggests a more complex relationship between DIN concentrations, seasonality, and discharge, given that  
12 peak DIN concentrations were also observed during low flow conditions (Fig. 6b and 6c). In particular, a prominent  $\text{NH}_4^+$   
13 peak during the JJAS dry season of 2013 occurred in conjunction with peaks in POC and PN, and might be attributed to in-  
14 situ processing of the dry season organic matter inputs from large herbivores in the lower basin, as outlined above. Similarly,  
15 a prominent peak in  $\text{NO}_3^-$  was observed during the JF dry season, for which no clear explanation exists. Despite this, our flux  
16 estimates suggest that the annual DIN and PN export predominantly occurs during the wet seasons as a result of the elevated  
17 discharge conditions, and with the consistent enrichment of the PN pool in  $^{15}\text{N}$  (Fig. 3d) relative to the  $\delta^{15}\text{N}$  composition of  
18 biologically fixed N (i.e.  $\sim 0\text{\textperthousand}$  to  $+2\text{\textperthousand}$ ), supports the analysis of Marwick et al. (2014a) that anthropogenic inputs impart  
19 significant influence on the cycling of N in the A-G-S basin and the export budget of N from the Sabaki River to the coastal  
20 zone.

21 The Global Nutrient Export from Watersheds 2 (NEWS2; see Mayorga et al. (2010)) provides flux and yield estimates for  
22 TSM and particulate and dissolved fractions of organic and inorganic forms of C, N, and P for  $> 6000$  river basins through  
23 hybrid empirical and conceptual based models relying on single and multiple linear regressions and single-regression  
24 relationships. Comparatively, our flux estimates are in general considerably lower than the NEWS2 estimates (Table 1),  
25 except for the dissolved  $\text{PO}_4^{3-}$  pool. There are at least three likely explanations for these over estimates. Firstly, the basin  
26 area used in NEWS2 calculations is 2.5-fold greater than our estimate, and given the flux estimates of Mayorga et al. (2010)  
27 are also a function of basin area, it is understandable there will be considerable over-estimation by the model. Secondly, the  
28 TSM sub-model is grounded in datasets of observed conditions (generally not impacted by extensive flow regulation) and  
29 independent factors including precipitation, a relief index, dominant lithology, wetland rice and marginal grassland extent,  
30 whereas the export of particulate forms of C, N, and P are reliant on empirical relationships between contents of TSM and  
31 POC (Ludwig et al., 1996) and POC and PN (Ittekkot and Zhang, 1989), and a relationship for particulate phosphorus export  
32 based on POC load developed by Beusen et al. (2005). We suggest these relationships may not extrapolate well to a basin so  
33 severely impacted by anthropogenic inputs as the A-G-S system. Thirdly, export of dissolved fractions is built upon an  
34 empirical dataset from 131 global river basins, though this includes only nine African basins, compared to 45 basins for



1 North America and 36 basins for Europe for example, and hence the relationships developed from these datasets will be  
2 biased towards conditions observed in these regions and not necessarily reflective of African systems. Additionally, the  
3 NEWS2 model only takes into account contributions from sewage when areas are connected to sewage systems (i.e. point  
4 source inputs), which is not the case for 1.5 million residents of Nairobi, and may explain the major underestimation of the  
5 dissolved  $\text{PO}_4^{3-}$  flux.

## 6 **4.2 Greenhouse gases**

7 The combination of high frequency sampling and long-term monitoring of dissolved  $\text{CH}_4$  and  $\text{N}_2\text{O}$  concentrations in the  
8 rivers of Africa remain scarce (Borges et al., 2015a). The average and median concentrations of  $\text{CH}_4$  in the Sabaki River  
9 ( $483 \pm 530 \text{ nmol L}^{-1}$  and  $311 \text{ nmol L}^{-1}$ , respectively;  $n = 50$ ) often exceeded observations in other rivers of Africa, including  
10 the mid-and lower-Tana River ( $54 - 387 \text{ nmol L}^{-1}$ ; Bouillon et al. (2009)), the Comoé, Bia and Tanoé rivers of Ivory Coast  
11 ( $48 - 870 \text{ nmol L}^{-1}$ ; Koné et al. (2010)), and the Oubangui River of Central African Republic ( $74 - 280 \text{ nmol L}^{-1}$ ; Bouillon  
12 et al. (2012)). On a seasonal basis,  $\text{CH}_4$  concentrations tended to rise and fall with discharge (Fig. 7a), opposite to  
13 observations in the Oubangui and Ivory Coast rivers where highest concentrations are observed during low flow periods and  
14 decrease as discharge increases (Koné et al., 2010; Bouillon et al., 2012), and is likely linked to the increased supply of  
15 organic waste primed for decomposition from Nairobi. On the other hand, the highest peaks ( $1857 - 2838 \text{ nmol L}^{-1}$ ; 85171 –  
16 135111% saturation) were observed over the dry JJAS dry seasons of 2012 and 2013, their timing coinciding with the peaks  
17 in POC, PN, and  $\text{NH}_4^+$  previously discussed and attributed to large mammalian inputs, and we suggest these short-lived dry  
18 season  $\text{CH}_4$  peaks likely represent the decomposition of these mammalian-mediated terrestrial subsidies.  $\text{CH}_4$  showed two  
19 seasonal peaks, one during high water and another at the end of the low water period. The peak of  $\text{CH}_4$  during high water might be  
20 related to the increased connectivity between river and wetlands such as floodplains as reported in the Zambezi river (Teodoru et  
21 al., 2015), and in the Oubangui (Bouillon et al. 2012; 2014). The peak of  $\text{CH}_4$  at the end of the dry season is obviously unrelated to  
22 interaction with wetlands since at this period river and floodplains are hydrologically disconnected. We hypothesize that this  
23 increase of  $\text{CH}_4$  is related to the combination of increase water residence time and the additional inputs of organic matter from  
24 hippopotami. Indeed, they aggregate during low flow in river pools and river banks leading to a substantial input of organic matter  
25 (Subalusky et al., 2015), that we hypothesize leads to enhanced in-stream  $\text{CH}_4$  production. During high-water period, the  
26 hippopotami disperse across the landscape, presumably having a lower impact on river water biogeochemistry. Indeed, during the  
27 low water period  $\text{O}_2$  decreased in 2011, although the  $\text{CH}_4$  increase was modest. However, the marked increase of  $\text{CH}_4$  at the end of  
28 the 2013 dry season was mirrored by a distinct decrease of  $\text{O}_2$  saturation level from ~100% to ~20%. Although we provide no flux  
29 estimates, these elevated concentrations relative to observations in other African river systems at least hint that the A-G-S  
30 river system may be a relatively significant source of  $\text{CH}_4$  outgassing at the local scale.

31 Nitrous oxide in rivers is sourced from either nitrification or denitrification, and although the interest in  $\text{N}_2\text{O}$  is growing due  
32 to its recognition as a significant contributor to radiative forcing (Hartmann et al., 2013) and as a major ozone depleting  
33 substance (Ravishankara et al., 2009), relatively limited datasets are available for rivers (see Baulch et al. (2011); Beaulieu et



1 al. (2011); Marzadri et al. (2017)) and very few for tropical systems specifically (see Guérin et al. (2008); Bouillon et al.  
2 (2012); Borges et al. (2015a)). We observe similar seasonal patterns in the Sabaki River as those observed by Bouillon et al.  
3 (2012) in the Oubangui River, with concentrations during low flow conditions typically hovering between  $\sim 5 - 6$  nmol L $^{-1}$   
4 (Fig. 7b) and increasing as high flow conditions approach, though our peak concentration (26.6 nmol L $^{-1}$ ; 463% saturation)  
5 is considerably higher than that reported for the largely pristine Oubangui River basin (9.6 nmol L $^{-1}$ ; 165% saturation), with  
6 this pattern reflecting well the concentrations observed at the monitoring station during the basin-wide campaigns of JJAS  
7 dry season (6.3 nmol L $^{-1}$ ; 116% saturation) and OND wet season (15.8 nmol L $^{-1}$ ; 274% saturation). The seasonal pattern  
8 reported from these African rivers is unique compared to temperate rivers, where the opposite pattern is more typical (Cole  
9 and Caraco, 2001b; Beaulieu et al., 2011). Given the reported correlation between N<sub>2</sub>O and NO<sub>3</sub><sup>-</sup> concentrations in various  
10 river systems (Baulch et al., 2011; Beaulieu et al., 2011), including three from Africa (Borges et al., 2015a), and that basin-  
11 wide data shows gradually increasing concentrations of NO<sub>3</sub><sup>-</sup> from  $\sim 179$   $\mu$ mol L $^{-1}$  to 538  $\mu$ mol L $^{-1}$  over the 200 km reach  
12 directly upstream of the monitoring site during the OND wet season (see Marwick et al. (2014a)), we make a first  
13 assumption that the elevated N<sub>2</sub>O concentrations during the wet season may be driven by upstream nitrification of the  
14 wastewater inputs identified in Marwick et al. (2014a).

#### 15 4.3 Future outlook

16 The biogeochemical cycles and budgets of the Athi-Galana-Sabaki river system have been considerably perturbed by the  
17 introduction of European agricultural practises in the early 20<sup>th</sup> century and the expanding population of Nairobi living with  
18 inadequate waste water facilities (Van Katwijk et al., 1993; Fleitmann et al., 2007). These factors have had considerable  
19 impact on riverine sediment loads (Fleitmann et al., 2007), instream nutrient cycling (Marwick et al., 2014a), and near-shore  
20 marine ecosystems in the vicinity of the Sabaki outlet (Giesen and van de Kerkhof, 1984; Van Katwijk et al., 1993). Recent  
21 modelling of nutrient export to the coastal zone of Africa to the year 2050 foreshadows continued perturbation to these  
22 ecosystems, with the extent dependant on the land management pathway followed and mitigation strategies emplaced (Yasin  
23 et al., 2010). Although suspended sediment fluxes are estimated to decrease over Africa in the coming 40 years, the  
24 projected increase in dissolved forms of N and P and decreases in particulate forms of C, N, P as well as dissolved OC  
25 (Yasin et al., 2010) will further augment nutrient stoichiometry within the inland waters of the A-G-S system.

26 Although no large reservoirs have been developed within the A-G-S basin, approval has been given for the construction of  
27 the Thwake multi-purpose dam on the Athi River, though commencement has been delayed by tender approval for the  
28 project. The total surface area is expected to be in the vicinity of 29 km $^2$ , and the completed reservoir can be expected to  
29 have a considerable impact on the downstream geomorphology and biogeochemistry of the river, as experienced in the  
30 neighbouring reservoir-regulated Tana River (see Adams and Hughes (1986); Maingi and Marsh, 2002; Bouillon et al.  
31 (2009); Tamooh et al. (2012), Tamooh et al. (2014); Okuku et al., (2016)). Given lakes and reservoirs enhance the cycling  
32 and removal of nutrients due to their ability to prolong material residence times and subsequently enhance particle settling  
33 and in-situ processing (Wetzel, 2001; Harrison et al., 2009), in addition to suggestions that GHG emissions from lentic



1 systems of the tropics may be disproportionately large relative to temperate and northern latitude systems (Aufdenkampe et  
2 al., 2011; Bastviken et al., 2011; Raymond et al., 2013; Borges et al. 2015b), it is reasonable to assume the planned reservoir  
3 on the Athi River will become a biogeochemical hotspot for the processing, storage and removal of upstream anthropogenic-  
4 driven nutrient loads. The datasets presented within Marwick et al. (2014a) and here provide critical base-line data for future  
5 research initiatives in the A-G-S system, not only to assess the evolving fluvial biogeochemistry of the basin in response to a  
6 newly constructed tropical reservoir, but importantly, to review the influence flow regulation has on nutrient and suspended  
7 sediment fluxes to the coastal zone, and subsequently the health and biodiversity of the Malindi-Watamu Marine National  
8 Park ecosystem.

## 9 **Supplementary Materials**

10 Raw data and additional figures referred to in-text are included in the Supplementary Materials.

## 11 **Team list**

12 Trent R. Marwick  
13 Fredrick Tamoooh  
14 Bernard Ogwoka  
15 Alberto V. Borges  
16 François Darchambeau  
17 Steven Bouillon

## 18 **Author Contributions**

19 TRM: lead author, conceived research, performed field sampling, performed sample and data analysis, wrote paper. FT:  
20 performed field sampling and sample analysis. BO: performed field sampling. AVB: conceived research, performed sample  
21 analysis, wrote paper. FD: performed sample analysis. SB: conceived research, performed sample and data analysis, wrote  
22 paper.

## 23 **Competing Interests**

24 The authors declare that they have no conflict of interest.

## 25 **Acknowledgements.**

26 Funding for this work was provided by the European Research Council (ERC-StG 240002, AFRIVAL,  
27 <http://ees.kuleuven.be/project/aftrival/>), and by the Research Foundation Flanders (FWO-Vlaanderen, project G.0651.09). We  
28 thank Z. Kelemen (KU Leuven), P. Salaets (KU Leuven), and M.-V. Commarieu (ULg) for technical and laboratory  
29 assistance, and J. Ngilu and W.R.M.A. (Water Resource Management Authority, Machakos, Kenya) for providing the



1 discharge data. Thanks also to Christopher Still and Rebecca Powell for providing the GIS data layers of their isoscape  
2 models. A. V. Borges is a senior research associate at the FRS-FNRS (Belgium).

### 3 References

- 4 Abrantes, K. G., Barnett, A., Marwick, T. R., and Bouillon, S.: Importance of terrestrial subsidies for estuarine food webs in contrasting  
5 East African catchments, *Ecosphere* 4(1), Article 14, doi:10.1890/ES12-00322.1, 2013.
- 6 Abril, G., Commarieu, M. V., and Guérin, F.: Enhanced methane oxidation in an estuarine turbidity maximum. *Limnol. Oceanogr.*, 52(1),  
7 470–475, 2007.
- 8 Abril, G., Martinez, J.-M., Artigas, L. F., Moreira-Turcq, P., Benedetti, M. F., Vidal, L., Meziane, T., Kim, J.-H., Bernardes, M. C.,  
9 Savoye, N., Deborde, J., Albéric, P., Souza, M. F. L., Souza, E. L., Roland, F.: Amazon River carbon dioxide outgassing fuelled by  
10 wetlands, *Nature*, 505, 395–398, 2014.
- 11 Adams, W. M., and Hughes, F. M.: The environmental effects of dam construction in tropical Africa: impacts and planning procedures,  
12 *Geoforum*, 17(3), 403–410, doi:10.1016/0016-7185(86)90007-2, 1986.
- 13 Aitkenhead, J. A., and McDowell, W. H.: Soil C: N ratio as a predictor of annual riverine DOC flux at local and global scales, *Global  
14 Biogeochem. Cy.*, 14(1), 127–138, doi:10.1029/1999GB900083, 2000.
- 15 Aravena, R., Evans, M. L., and Cherry, J. A.: Stable isotopes of oxygen and nitrogen in source identification of nitrate from septic systems,  
16 *Ground Water*, 31(2), 180–186, doi:10.1111/j.1745-6584.1993.tb01809.x, 1993.
- 17 Aufdenkampe, A. K., Mayorga, E., Raymond, P. A., Melack, J. M., Doney, S. C., Alin, S. R., Aalto, R. E., and Yoo, K.: Riverine coupling  
18 of biogeochemical cycles between land, oceans, and atmosphere, *Front. Ecol. Environ.*, 9(1), 53–60, doi:10.1890/100014, 2011.
- 19 Bastviken, D., Tranvik, L. J., Downing, J. A., Crill, P. M., and Enrich-Prast, A.: Freshwater methane emissions offset the continental  
20 carbon sink, *Science*, 331(6073), 50, doi:10.1126/science.1196808, 2011.
- 21 Battin, T. J., Kaplan, L. A., Findlay, S., Hopkinson, C. S., Marti, E., Packman, A. I., Newbold, J. D., and Sabater, F.: Biophysical controls  
22 on organic carbon fluxes in fluvial networks, *Nature Geosci.*, 1, 95–100, doi: 10.1038/ngeo101, 2008.
- 23 Battin, T. J., Luyssaert, S., Kaplan, L. A., Aufdenkampe, A. K., Richter, A., and Tranvik, L. J.: The boundless carbon cycle, *Nat. Geosci.*,  
24 2(9), 598–600, doi:10.1038/ngeo618, 2009.
- 25 Baulch, H. M., Schiff, S. L., Maranger, R., and Dillon, P. J.: Nitrogen enrichment and the emission of nitrous oxide from streams, *Global  
26 Biogeochem. Cy.*, 25, GB4013, doi:10.1029/2011GB004047, 2011.
- 27 Beaulieu, J. J., Tank, J. L., Hamilton, S. K., Wollheim, W. M., Hall Jr, R. O., Mulholland, P. J., Peterson, B. J., Ashkenas, L. R., Cooper,  
28 L. W., Dahm, C. N., Dodds, W. K., Grimm, N. B., Johnson, S. L., McDowell, W. H., Poole, G. C., Valett, H. M., Arango, C. P., Bernot,  
29 M. J., Burgin, A. J., Crenshaw, C. L., Helton, A. M., Johnson, L. T., O'Brien, J. M., Potter, J. D., Sheibley, R. W., Sobota, D. J., and  
30 Thomas, S. M.: Nitrous oxide emission from denitrification in stream and river networks, *P. Natl. Acad. Sci. USA*, 108(1), 214–219,  
31 doi:10.1073/pnas.1011464108, 2011.
- 32 Beusen, A. H. W., Dekkers, A. L. M., Bouwman, A. F., Ludwig, L., and Harrison, J.: Estimation of global river transport of sediments and  
33 associated particulate C, N, and P, *Global Biogeochem. Cy.*, 19, GB4S05, doi:10.1029/2005GB002453, 2005.
- 34 Bird, M. I., and Pousai, P.: Variations of  $\delta^{13}\text{C}$  in the surface soil organic carbon pool, *Global Biogeochem. Cy.*, 11(3), 313–322,  
35 doi:10.1029/97GB01197, 1997.
- 36 Bird, M. I., Fyfe, W. S., Pinheiro-Dick, D., and Chivas, A. R.: Carbon isotope indicators of catchment vegetation in the Brazilian Amazon,  
37 *Global Biogeochem. Cy.*, 6(3), 293–306, doi:10.1029/92GB01652, 1992.
- 38 Bird, M. I., Giresse, P., and Chivas, A. R.: Effect of forest and savanna vegetation on the carbon-isotope composition from the Sanaga  
39 River, *Cameroon, Limnol. Oceanogr.*, 39(8), 1845–1854, doi:10.4319/lo.1994.39.8.1845, 1994.
- 40 Bird, M. I., Giresse, P., and Ngos, S.: A seasonal cycle in the carbon-isotope composition of organic carbon in the Sanaga River,  
41 *Cameroon, Limnol. Oceanogr.*, 43(1), 143–146, doi:10.4319/lo.1998.43.1.0143, 1998.
- 42 Borges, A. V., Darchambeau, F., Teodoro, C. R., Marwick, T. R., Tambooh, F., Geeraert, N., Omengo, F., Guérin, F., Lambert, T., Morana,  
43 C., Okuku, E., and Bouillon, S.: Globally significant greenhouse-gas emissions from African inland waters, *Nature Geoscience*, 8, 637–  
44 642, doi:10.1038/ngeo2486, 2015a.



- 1 Borges, A. V., Abril, G., Darchambeau, F., Teodoru, C. R., Deborde, J., Vidal, L. O., Lambert, T., and Bouillon, S.: Divergent biophysical  
2 controls of aquatic CO<sub>2</sub> and CH<sub>4</sub> in the World's two largest rivers, *Scientific Reports*, 5:15614, doi: 10.1038/srep15614, 2015b.
- 3 Bouillon, S., Kornthauer, M., Baeyens, W., and Dehairs, F.: A new automated setup for stable isotope analysis of dissolved organic  
4 carbon, *Limnol. Oceanogr.-Meth.*, 4, 216–226, 2006.
- 5 Bouillon, S., Abril, G., Borges, A. V., Dehairs, F., Govers, G., Hughes, H. J., Merckx, R., Meysman, F. J. R., Nyunja, J., Osburn, C., and  
6 Middelburg, J. J.: Distribution, origin and cycling of carbon in the Tana River (Kenya): a dry season basin-scale survey from headwaters to  
7 the delta, *Biogeosciences*, 6, 2475–2493, doi:10.5194/bgd-6-5959-2009, 2009.
- 8 Bouillon, S., Yambélé, A., Spencer, R. G. M., Gillikin, D. P., Hernes, P. J., Six, J., Merckx, R., and Borges, A. V.: Organic matter sources,  
9 fluxes and greenhouse gas exchange in the Oubangui River (Congo River basin), *Biogeosciences*, 9, 2045–2062, doi:10.5194/bg-9-2045-  
10 2012, 2012.
- 11 Bouillon, S., Yambélé, A., Gillikin, D. P., Teodoru, C., Darchambeau, F., Lambert, T., and Borges, A. V.: Contrasting biogeochemical  
12 characteristics of the Oubangui River and tributaries (Congo River Basin), *Scientific Reports*, 4, Art. 5402, doi:10.1038/srep05402, 2014.
- 13 Brunet, F., Dubois, K., Veizer, J., Nkoue Ndondo, G. R., Ndam Ngoupayou, J. R., Boeglin, J. L., and Probst, J. L.: Terrestrial and fluvial  
14 carbon fluxes in a tropical watershed: Nyong basin, Cameroon, *Chem. Geol.*, 265(3-4), 563–572, doi:10.1016/j.chemgeo.2009.05.020,  
15 2009.
- 16 Buontempo, C., Mathison, C., Jones, R., Williams, K., Wang, C., and McSweeney, C.: An ensemble climate projection for Africa, *Clim.  
17 Dyn.*, 44(7–8), 2097–2118, doi: 10.1007/s00382-014-2286-2, 2015.
- 18 Champion, A. M.: Soil erosion in Africa, *Geogr. J.*, 82(2), 130–139, doi:10.2307/1785660, 1933.
- 19 Ciais, P., Bombelli, A., Williams, M., Piao, S. L., Chave, J., Ryan, C. M., Henry, M., Breden, P., and Valentini, R.: The carbon balance of  
20 Africa: synthesis of recent research studies, *Philos. T. Roy. Soc. A*, 369(1934), 2038–2057, doi:10.1098/rsta.2010.0328, 2011.
- 21 Ciais, P., Sabine, C., Bala, G., Bopp, L., Brovkin, V., Canadell, J., Chhabra, A., DeFries, R., Galloway, J., Heimann, M., Jones, C., Le  
22 Quéré, C., Myneni, R. B., Piao, S., and Thornton, P.: Carbon and Other Biogeochemical Cycles, *Climate Change 2013: The Physical  
23 Science Basis. Contribution of Working Group I to the Fifth Assessment Report of the Intergovernmental Panel on Climate Change*  
24 [Stocker, T.F., D. Qin, G.-K. Plattner, M. Tignor, S.K. Allen, J. Boschung, A. Nauels, Y. Xia, V. Bex and P.M. Midgley (eds.)].  
25 Cambridge University Press, Cambridge, United Kingdom and New York, NY, USA, pp. 465–570, doi:10.1017/CBO9781107415324.015,  
26 2013.
- 27 Cole, J. J., and Caraco, N. F.: Carbon in catchments: connecting terrestrial carbon losses with aquatic metabolism, *Mar. Freshwater Res.*,  
28 52(1), 101–110, doi: 10.1071/MF00084, 2001a.
- 29 Cole, J. J., and Caraco, N. F.: Emissions of nitrous oxide (N<sub>2</sub>O) from a tidal, freshwater river, the Hudson River, New York, *Environ. Sci.  
30 Technol.*, 35, 991–996, 2001b.
- 31 Cole, J. J., Caraco, N. F., Kling, G. W., and Kratz, T. K.: Carbon dioxide supersaturation in the surface waters of lakes, *Science*,  
32 265(5178), 1568–1570, doi:10.1126/science.265.5178.1568, 1994.
- 33 Cole, J. J., Prairie, Y. T., Caraco, N. F., McDowell, W. H., Tranvik, L. J., Striegl, R. G., Duarte, C. M., Kortelainen, P., Downing, J. A.,  
34 Middelburg, J. J., and Melack, J.: Plumbing the global carbon cycle: Integrating inland waters into the terrestrial carbon budget,  
35 *Ecosystems*, 10(1), 171–184, doi:10.1007/s10021-006-9013-8, 2007.
- 36 Coynel, A., Seyler, P., Etcheber, H., Meybeck, M., and Orange, D.: Spatial and seasonal dynamics of total suspended sediment and  
37 organic carbon species in the Congo River, *Global Biogeochem. Cy.*, 19(4), GB4019, doi:10.1029/2004GB002335, 2005.
- 38 Dafe, F.: No business like slum business? The political economy of the continued existence of slums: a case study of Nairobi, DESTIN:  
39 Development Studies Institute, Working Paper Series, No. 09–98, 2009.
- 40 Delft Hydraulics: Malindi Bay Pollution II, Field measurements and recommendations, Report R611, Delft Hydraulics Laboratory, The  
41 Netherlands, 1970.
- 42 Dosio, A., and Panitz, H. J.: Climate change projections for CORDEX-Africa with COSMO-CLM regional climate model and differences  
43 with the driving global climate models, *Clim. Dyn.*, 46(5–6), 1599–1625, doi:10.1007/s00382-015-2664-4, 2016.
- 44 Dunne, T.: Sediment yield and land use in tropical catchments, *J. Hydrol.*, 42(3-4), 281–300, doi:10.1016/0022-1694(79)90052-0, 1979.
- 45 Finn, D.: Land use and abuse in the East African region, *Ambio* 12(6), 296–301, 1983.



- 1 Fleitmann, D., Dunbar, R. B., McCulloch, M., Mudelsee, M., Vuille, M., McClanahan, T. R., Cole, J. E., and Eggins, S.: East African soil  
2 erosion recorded in a 300 year old coral colony from Kenya, *Geophys. Res. Lett.*, 34(4), L04401, doi:10.1029/2006GL028525, 2007.
- 3 Geeraert, N., Omengo, F. O., Tamooh, F., Marwick, T. R., Borges, A. V., Govers, G., and Bouillon, S.: Seasonal and inter-annual  
4 variations in carbon fluxes in a tropical river system (Tana River, Kenya), *Aquatic Sciences*, in review.
- 5 Giesen, W., and Van de Kerkhof, K.: The impact of river discharges on the Kenya coral reef ecosystem - the physical processes, Part II:  
6 Effect on the Malindi-Watamu coastal environment, Report no. 194, Laboratory of Aquatic Ecology, Catholic University, Nijmegen, The  
7 Netherlands, 1984.
- 8 Gillikin, D. P., and Bouillon, S.: Determination of  $\delta^{18}\text{O}$  of water and  $\delta^{13}\text{C}$  of dissolved inorganic carbon using a simple modification of  
9 an elemental analyser-isotope ratio mass spectrometer: an evaluation, *Rapid Commun. Mass Sp.*, 21(8), 1475–1478,  
10 doi:10.1002/rcm.2968, 2007.
- 11 Grey, J., and Harper, D. M.: Using stable isotope analyses to identify allochthonous inputs to Lake Naivasha mediated via the  
12 hippopotamus gut, *Isotopes Environ. Health Stud.*, 38(4), 245–250, 2002.
- 13 Guérin, F., Abril, G., Tremblay, A., and Delmas, R.: Nitrous oxide emissions from tropical hydroelectric reservoirs, *Geophys. Res. Lett.*,  
14 35, L06404, doi:10.1029/2007GL033057, 2008.
- 15 Hamilton, S. K.: Biogeochemical implications of climate change for tropical rivers and floodplains, *Hydrobiologia*, 657(1), 19–35,  
16 doi:10.1007/s10750-009-0086-1, 2010.
- 17 Hamilton, S. K., Sippel, S., Calheiros, D. F., and Melack, J. F.: An anoxic event and other biogeochemical effects of the Pantanal wetland  
18 on the Paraguay river, *Limnol. Oceanogr.*, 4(2), 257–272, 1997.
- 19 Harrison, J. A., Maranger, R. J., Alexander, R. B., Giblin, A. E., Jacinthe, P. A., Mayorga, E., Seitzinger, S. P., Sobota, D. J., and  
20 Wollheim, W. M.: The regional and global significance of nitrogen removal in lakes and reservoirs, *Biogeochemistry*, 93(1-2), 143–157,  
21 doi:10.1007/s10533-008-9272-x, 2009.
- 22 Hartmann, D. L., Klein Tank, A. M. G., Rusticucci, M., Alexander, L. V., Brönnimann, S., Charabi, Y., Dentener, F. J., Dlugokencky, E.  
23 J., Easterling, D. R., Kaplan, A., Soden, B. J., Thorne, P. W., Wild, M., and Zhai, P. M.: Observations: Atmosphere and Surface, Climate  
24 Change 2013: The Physical Science Basis. Contribution of Working Group I to the Fifth Assessment Report of the Intergovernmental  
25 Panel on Climate Change [Stocker, T.F., D. Qin, G.-K. Plattner, M. Tignor, S.K. Allen, J. Boschung, A. Nauels, Y. Xia, V. Bex and P.M.  
26 Midgley (eds.)]. Cambridge University Press, Cambridge, United Kingdom and New York, NY, USA, 2013.
- 27 Hedges, J. I., Clark, W. A., Quay, P. D., Richey, J. E., Devol, A. H., and Santos, U. de M.: Compositions and fluxes of particulate organic  
28 material in the Amazon River, *Limnol. Oceanogr.*, 31(4), 717–738, 1986.
- 29 IPCC: Climate Change 2013: The Physical Science Basis. Contribution of Working Group I to the Fifth Assessment Report of the  
30 Intergovernmental Panel on Climate Change [Stocker, T.F., D. Qin, G.-K. Plattner, M. Tignor, S.K. Allen, J. Boschung, A. Nauels, Y. Xia,  
31 V. Bex and P.M. Midgley (eds.)], Cambridge University Press, Cambridge, United Kingdom and New York, NY, USA, 1535 pp,  
32 doi:10.1017/CBO9781107415324, 2013.
- 33 Ittekkot, V., and Zhang, S.: Pattern of particulate nitrogen transport in world rivers, *Global Biogeochem. Cy.*, 3, 383–391,  
34 doi:10.1029/GB003i004p00383, 1989.
- 35 Kitheka, J. U.: River sediment supply, sedimentation and transport of the highly turbid sediment plume in Malindi Bay, Kenya, *J. Geogr.  
Sci.*, 23(3), 465–489, doi:10.1007/s11442-013-1022-x, 2013.
- 37 Kitheka, J. U., Obiero, M., and Nthenge, P.: River discharge, sediment transport and exchange in the Tana estuary, Kenya, *Estuar. Coast.  
Shelf S.*, 63, 455–468, doi:10.1016/j.ecss.2004.11.011, 2005.
- 39 Kithia, S. M.: Land use changes and their effects on sediment transport and soil erosion within the Athi drainage basin, Kenya, *IAHS-AISH P.*,  
40 245, 145–150, 1997.
- 41 Kithia, S. M., and Wambua, B. N.: Temporal changes of sediment dynamics within the Nairobi River sub-basins between 1998-2006 time  
42 scale, Kenya, *Annals of Warsaw University of Life Sciences – SGGW, Land Reclamation*, 42(1), doi:10.2478/v10060-008-0060-z, 2010.
- 43 Kling, G. W., Kipphut, G. W., and Miller, M. C.: Arctic lakes and streams as gas conduits to the atmosphere: implications for tundra  
44 carbon budgets, *Science*, 251(4991), 298–301, doi:10.1126/science.251.4991.298, 1991.
- 45 Koné Y. J. M., Abril, G., Delille, B., and Borges, A. V.: Seasonal variability of methane in the rivers and lagoons of Ivory Coast (West  
46 Africa), *Biogeochemistry*, 100(1-3), 21–37, doi:10.1007/s10533-009-9402-0, 2010.



- 1 Lehner, B., Verdin, K., Jarvis, A.: HydroSHEDS Technical Documentation, World Wildlife Fund US, Washington, DC.  
2 <http://hydrosheds.cr.usgs.gov>, 2006.
- 3 Lesack, L. F. W., Hecky, R. E., and Melack, J. M.: Transport of carbon, nitrogen, phosphorous and major solutes in the Gambia River,  
4 West Africa, *Limnol. Oceanogr.*, 29(4), 816–830, doi:10.4319/lo.1984.29.4.0816, 1984.
- 5 Likens, G. E., Mackenzie, F. T., Richey, J. E., Sedell, J. R., and Turekian, K. K. [eds.]: Flux of organic carbon by rivers to the ocean.  
6 Conf. 8009140. DOE, Office Energy Res., Washington, D.C., USA, 1981.
- 7 Ludwig, W., Probst, J. L., and Kempe, S.: Predicting the oceanic input of organic carbon by continental erosion, *Global Biogeochem. Cy.*,  
8 10(1), 23–41, doi:10.1029/95GB02925, 1996.
- 9 Maingi, J. K., and Marsh, S. E.: Quantifying hydrologic impacts following dam construction along the Tana River, Kenya, *J. Arid  
10 Environ.*, 50(1), 53–79, doi:10.1006/jare.2000.0860, 2002.
- 11 Mariotti, A., Gadel, F., and Giresse, P.: Carbon isotope composition and geochemistry of particulate organic matter in the Congo River  
12 (Central Africa): application to the study of Quaternary sediments off the mouth of the river, *Chem. Geol.: Isotope Geoscience section*,  
13 86(4), 345–357, doi:10.1016/0168-9622(91)90016-P, 1991.
- 14 Marwick, T. R., Tamoooh, F., Ogwoka, B., Teodoru, C. R., Borges, A. V., Darchambeau, F., and Bouillon, S.: Dynamic seasonal nitrogen  
15 cycling in response to anthropogenic N-loading in a tropical catchment, Athi–Galana–Sabaki River, Kenya, *Biogeosciences*, 11, 443–460,  
16 doi:10.5194/bg-11-443-2014, 2014a.
- 17 Marwick, T. R., Borges, A. V., Van Acker, K., Darchambeau, F., and Bouillon, S.: Disproportionate Contribution of Riparian Inputs to  
18 Organic Carbon Pools in Freshwater Systems, *Ecosystems*, 17(6), 974–989, doi:10.1007/s10021-014-9772-6, 2014b.
- 19 Marzadri, A., Dee, M. M., Tonina, D., Bellin, A., and Tank, J. L.: Role of surface and subsurface processes in scaling N<sub>2</sub>O emissions along  
20 riverine networks, *P. Natl. Acad. Sci.*, 114(17), 4330–4335, 10.1073/pnas.1617454114, 2017.
- 21 Masese, F. O., Abrantes, K. G., Gettel, G. M., Bouillon, S., Irvine, K., and McClain, M. E.: Are large herbivores vectors of terrestrial  
22 subsidies for riverine food webs?, *Ecosystems*, 18(4), 686–706, doi:10.1007/s10021-015-9859-8, 2015.
- 23 Mayaux, P., Bartholomé, E., Fritz, S., and Belward, A.: A new land-cover map of Africa for the year 2000, *Journal of Biogeography*, 31,  
24 861–877. doi:10.1111/j.1365-2699.2004.01073.x, 2004.
- 25 Mayorga, E., Seitzinger, S. P., Harrison, J. A., Dumont, E., Beusen, A. H. W., Bouwman, A. F., Fekete, B. M., Kroeze, C., and Van  
26 Drecht, A.: Global nutrient export from WaterSheds 2 (NEWS 2): model development and implementation, *Environ. Modell. Softw.*,  
27 25(7), 837–853, doi:10.1016/j.envsoft.2010.01.007, 2010.
- 28 Meehl, G. A., Stocker, T. F., Collins, W. D., Friedlingstein, P., Gaye, A. T., Gregory, J. M., Kitoh, A., Knutti, R., Murphy, J. M., Noda,  
29 A., Raper, S. C. B., Watterson, I. G., Weaver, A. J., and Zhao, Z.-C.: Global climate projections, in *Climate Change 2007: The Physical  
30 Science Basis. Contribution of Working Group I to the Fourth Assessment Report of the Intergovernmental Panel on Climate Change*,  
31 edited by S. Solomon et al., Cambridge University Press, Cambridge, UK, 2007.
- 32 Meybeck, M.: Carbon, nitrogen, and phosphorus transport by world rivers, *Am. J. Sci.* 282, 401–450, doi:10.2475/ajs.282.4.401, 1982.
- 33 Milliman, J. D., and Farnsworth, K. L.: River discharge to the coastal ocean: a global synthesis, Cambridge University Press, New York,  
34 U.S.A., 2011.
- 35 Moore, S., Gauci, V., Evans, C. D., and Page, S. E.: Fluvial organic carbon losses from a Bornean blackwater river. *Biogeosciences*, 8(4),  
36 901–909, 2011.
- 37 Mogaka, H., Gichere, S., Davis, R., and Hirji, R.: Climate variability and water resources degradation in Kenya: improving water  
38 resources development and management, *World Bank Working Papers* 69, 2006.
- 39 Munyao, T. M., Tole, M. P., and Jungerius, P. D.: Sabaki River sediment transport and deposition in the Indian Ocean, *Research reports -  
40 African Studies Centre Leiden*, Netherlands, 2003.
- 41 Ngene, S., Ihwagi, F., Nzisa, M., Mukeka, J., Njumbi, S., and Omondi, P.: Total aerial census of elephants and other large mammals in the  
42 Tsavo-Mkomazi ecosystem, *Kenya Wildlife Service report*, 2011.
- 43 Oeurng, C., Sauvage, S., Coynel, A., Maneux, E., Etcheber, H., and Sanchez-Perez, M. J.: Fluvial transport of suspended sediment and  
44 organic carbon during flood events in a large agricultural catchment in southwest France, *Hydrol. Process.*, 25, 2365–2378,  
45 doi:10.1002/hyp.7999, 2011.



- 1 Okuku, E. O., Tole, M., Kiteresi, L. I., and Bouillon, S.: The response of phytoplankton and zooplankton to river damming in three  
2 cascading reservoirs of the Tana River, Kenya. *Lakes & Reservoirs: Research & Management*, 21(2), 114–132, 2016.
- 3 Ravishankara, A. R., Daniel, J. S., and Portmann, R. W.: Nitrous oxide (N<sub>2</sub>O): the dominant ozone-depleting substance emitted in the 21st  
4 century, *Science*, 326(5949), 123–125, doi:10.1126/science.1176985, 2009.
- 5 Raymond, P. A., Hartmann, J., Lauerwald, R., Sobek, S., McDonald, C., Hoover, M., Butman, D., Striegl, R., Mayorga, E., Humborg, C.,  
6 Kortelainen, P., Dürr, H., Meybeck, M., Ciais, P., and Guth, P.: Global carbon dioxide emissions from inland waters, *Nature*, 503, 355–  
7 359, doi:10.1038/nature12760, 2013.
- 8 Regnier, P., Friedlingstein, P., Ciais, P., Mackenzie, F. T., Gruber, N., Janssens, I. A., Laruelle, G. G., Lauerwald, R., Luyssaert, S.,  
9 Andersson, A. J., Arndt, S., Arnosti, C., Borges, A. V., Dale, A. W., Gallego-Sala, A., Goddérus, Y., Goossens, N., Hartmann, J., Heinze,  
10 C., Ilyina, T., Joos, F., LaRowe, D. E., Leifeld, J., Meysman, F. J. R., Munhoven, G., Raymond, P. A., Spahni, R., Suntharalingam, P., and  
11 Thullner, M.: Anthropogenic perturbation of the carbon fluxes from land to ocean, *Nat. Geosci.*, 6(8), 597–607, doi:10.1038/ngeo1830,  
12 2013.
- 13 Richey, J. E., Melack, J. M., Aufdenkampe, A. K., Ballester, V. M., and Hess, L. L.: Outgassing from Amazonian rivers and wetlands as a  
14 large tropical source of atmospheric CO<sub>2</sub>, *Nature*, 416, 617–620, doi:10.1038/416617a, 2002.
- 15 Rovira, A., and Batalla, R.: Temporal distribution of suspended sediment transport in a Mediterranean basin: The Lower Tordera (NE  
16 Spain), *Geomorphology*, 79, 58–71, doi:10.1016/j.geomorph.2005.09.016, 2006.
- 17 Subalusky, A. L., Dutton, C. L., Rosi-Marshall, E. J., and Post, D. M.: The hippopotamus conveyor belt: vectors of carbon and nutrients  
18 from terrestrial grasslands to aquatic systems in sub-Saharan Africa, *Freshwater Biology*, 60(3), 512–525, 2015.
- 19 Schlünz, B., and Schneider, R. R.: Transport of terrestrial organic carbon to the oceans by rivers: re-estimating flux and burial rates, *Int. J. Earth Sci.*, 88(4), 599–606, doi:10.1007/s005310050290, 2000.
- 21 Spitz, A., and Leenheer, J.: Dissolved organic carbon in rivers, p. 213–232. In E. T. Degens, S. Kempe, and J. E. Richey (eds.),  
22 *Biogeochemistry of Major World Rivers*, John Wiley and Sons, Chichester; England, 1991.
- 23 Stanley, E. H., Casson, N. J., Christel, S. T., Crawford, J. T., Loken, L. C., and Oliver, S. K.: The ecology of methane in streams and  
24 rivers: patterns, controls, and global significance, *Ecological Monographs*, 86(2), 146–171, doi: 10.1890/15-1027, 2016.
- 25 Still, C. J., and Powell, R. L.: Continental-scale distributions of vegetation stable carbon isotope ratios, in *Isoscapes*, edited by J. B. West  
26 et al., pp. 179–193, Springer, Netherlands, 2010.
- 27 Syvitski, J. P., Vörösmarty, C. J., Kettner, A. J., and Green, P.: Impact of humans on the flux of terrestrial sediment to the global coastal  
28 ocean, *Science*, 308(5720), 376–380, 2005.
- 29 Tamooch, F., Van den Meersche, K., Meysman, F., Marwick, T. R., Borges, A. V., Merckx, R., Dehairs, F., Schmidt, S., Nyunja, J., and  
30 Bouillon, S.: Distribution and origin of suspended sediments and organic carbon pools in the Tana River Basin, Kenya, *Biogeosciences*, 9,  
31 2905–2920, doi:10.5194/bgd-6-5959-2009, 2012.
- 32 Tamooch, F., Meysman, F. J., Borges, A. V., Marwick, T. R., Van Den Meersche, K., Dehairs, F., and Bouillon, S.: Sediment and carbon  
33 fluxes along a longitudinal gradient in the lower Tana River (Kenya), *J. Geophys. Res.-Biogeo.*, 119(7), 1340–1353,  
34 doi:10.1002/2013JG002358, 2014.
- 35 Teodoru, C. R., Nyoni, F. C., Borges, A., Darchambeau, F., Nyambe, I., and Bouillon, S.: Dynamics of greenhouse gases (CO<sub>2</sub>, CH<sub>4</sub>,  
36 N<sub>2</sub>O) along the Zambezi River and major tributaries, and their importance in the riverine carbon budget, *Biogeosciences*, 12(8), 2431–  
37 2453, 2015.
- 38 Tranvik, L. J., Downing, J. A., Cotner, J. B., Loiselle, S. A., Striegl, R. G., Ballatore, T. J., Dillon, P., Finlay, K., Fortino, K., Knoll, L. B.,  
39 Kortelainen, P. L., Kutser, T., Larsen, S., Laurion, I., Leech, D. M., McCallister, S. L., McKnight, D. M., Melack, J. M., Overholt, E.,  
40 Porter, J. A., Prairie, Y., Renwick, W. H., Roland, F., Sherman, B. S., Schindler, D. W., Sobek, S., Tremblay, A., Vanni, M. J., Verschoor,  
41 A. M., von Wachenfeldt, E., and Weyhenmeyer, G. A.: Lakes and reservoirs as regulators of carbon cycling and climate, *Limnol. Oceanogr.*, 54, 2298–2314, doi:10.4319/lo.2009.54.6\_part\_2.2298, 2009.
- 43 United Nations, Department of Economic and Social Affairs, Population Division: *World Population Prospects: The 2012 Revision*,  
44 Volume I: *Comprehensive Tables* ST/ESA/SER.A/336, 2013.
- 45 Valentini, R., Arneth, A., Bombelli, A., Castaldi, S., Cazzolla Gatti, R., Chevallier, F., Ciais, P., Grieco, E., Hartmann, J., Henry, M.,  
46 Houghton, R. A., Jung, M., Kutsch, W. L., Malhi, Y., Mayorga, E., Merbold, L., Murray-Tortarolo, G., Papale, D., Peylin, P., Poulter, B.,



- 1 Raymond, P. A., Santini, M., Sitch, S., Vaglio Laurin, G., van der Werf, G. R., Williams, C. A., and Scholes, R. J.: A full greenhouse  
2 gases budget of Africa: synthesis, uncertainties, and vulnerabilities, *Biogeosciences*, 11, 381–407, doi:10.5194/bg-10-8343-2013, 2014.
- 3 Van Katwijk, M., Meier, N. F., Loon, R. V., Hove, E. V., Giesen, W. B. J. T., Velde, G. V. D., and Hartog, C. D.: Sabaki river sediment  
4 load and coral stress: correlation between sediments and condition of the Malindi-Watamu reefs in Kenya (Indian Ocean), *Mar. Biol.*,  
5 117(4), 675–683, doi:10.1007/BF00349780, 1993.
- 6 Vanmaercke, M., Poesen, J., Broeckx, J., and Nyssen, J.: Sediment yield in Africa, *Earth-Sci. Rev.*, 136, 350–368,  
7 doi:10.1016/j.earscirev.2014.06.004, 2014.
- 8 Watermeyer, Legge, Piesold, Uhlman: Athi river basin pre-investment study. For: TARDA (Tana and Athi River Development Authority),  
9 Nairobi. Agrar & Hydrotechnik GmbH, Essen, 1981.
- 10 Weiss, R. F.: Determinations of carbon dioxide and methane by dual catalyst flame ionization chromatography and nitrous oxide by  
11 electron capture chromatography, *J. Chromatogr. Sci.*, 19(12), 611–616, doi:10.1093/chromsci/19.12.611, 1981.
- 12 Weiss, R. F., and Price, B. A.: Nitrous oxide solubility in water and seawater, *Mar. Chem.*, 8(4), 347–359, doi:10.1016/0304-  
13 4203(80)90024-9, 1980.
- 14 Wetzel, R. G.: *Limnology*, 3rd edn. Lake and river ecosystems, Academic Press, San Diego, 2001.
- 15 Widory, D., Petelet-Giraud, E., Negrel, P., and Ladouce, B.: Tracking the sources of nitrate in groundwater using coupled nitrogen and  
16 boron isotopes: a synthesis, *Environ. Sci. Technol.*, 39(2), 539–548, doi:10.1021/es0493897, 2005.
- 17 Yamamoto, S., Alcauskas, J. B., and Crozier, T. E.: Solubility of methane in distilled water and seawater, *J. Chem. Eng. Data*, 21(1), 78–  
18 80, doi: 10.1021/je60068a029, 1976.
- 19 Yasin, J. A., Kroese, C., and Mayorga, E.: Nutrients export by rivers to the coastal waters of Africa: past and future trends, *Global  
20 Biogeochem. Cy.*, 24(4), GB0A07, doi:10.1029/2009GB003568, 2010.
- 21 Zurbrügg, R., Suter, S., Lehmann, M. F., Wehrli, B., and Senn, D. B.: Organic carbon and nitrogen export from a tropical dam-impacted  
22 floodplain system, *Biogeosciences*, 10(1), 23–38, doi:10.5194/bg-10-23-2013, 2013.